

Improved Phenoxyalkylbenzimidazoles with Activity against *Mycobacterium tuberculosis* Appear to Target QcrB

N. Susantha Chandrasekera,[†] Bryan J. Berube,[†] Gauri Shetye,[†] Somsundaram Chettiar,[†] Theresa O'Malley,[†] Alyssa Manning,[†] Lindsay Flint,[†] Divya Awasthi,[†] Thomas R. Ioerger,[‡] James Sacchettini,[§] Thierry Masquelin,^{||} Philip A. Hipskind,^{||} Joshua Odingo,[†] and Tanya Parish^{*,†,||}

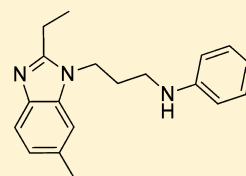
[†]TB Discovery Research, Infectious Disease Research Institute, 1616 Eastlake Avenue East, Seattle, Washington 98102, United States

[‡]Departments of Computer Science and Engineering and [§]Biochemistry and Biophysics, Texas A&M University, 301 Tarrow Street, College Station, Texas 77843, United States

^{||}Lilly Research Laboratories, 307 East Merrill Street, Indianapolis, Indiana 46285, United States

ABSTRACT: The phenoxy alkyl benzimidazoles (PABs) have good antitubercular activity. We expanded our structure–activity relationship studies to determine the core components of PABs required for activity. The most potent compounds had minimum inhibitory concentrations against *Mycobacterium tuberculosis* in the low nanomolar range with very little cytotoxicity against eukaryotic cells as well as activity against intracellular bacteria. We isolated resistant mutants against PAB compounds, which had mutations in either Rv1339, of unknown function, or *qcrB*, a component of the cytochrome *bc*₁ oxidase of the electron transport chain. QcrB mutant strains were resistant to all PAB compounds, whereas Rv1339 mutant strains were only resistant to a subset, suggesting that QcrB is the target. The discovery of the target for PAB compounds will allow for the improved design of novel compounds to target intracellular *M. tuberculosis*.

KEYWORDS: tuberculosis, benzimidazole, respiratory inhibitors, drugs



Wild type MIC ₉₀	0.056 μM
QcrB _{M342T} MIC ₉₀	4.1 μM
QcrB _{T313I} MIC ₉₀	8.7 μM
Intracellular IC ₉₀	0.028 μM
Raw Cytotoxicity TC ₅₀	> 50 μM

Mycobacterium tuberculosis was a leading cause of death by infectious disease in the world in 2015.¹ Contributing to over 1.4 million deaths and infecting an estimated one-third of the population, *M. tuberculosis* is a leading global health problem with major social and economic burdens.¹ Over the past decade, there has also been an alarming increase in multidrug-resistant (MDR-TB) and extensively drug-resistant (XDR-TB) strains that are refractory to conventional therapeutics.¹ Because of this, there is a dire need for novel drugs and preventatives to combat this disease.

The past few years have seen promising leads for new anti-tuberculosis drugs with several advancing to clinical trials. One series in the early stages of development, the phenoxy alkyl benzimidazoles (PAB), has shown good promise with minimum inhibitory concentrations (MICs) against *M. tuberculosis* in the nanomolar range, sterilizing activity under starvation conditions and low cytotoxicity against eukaryotic cells.²

In this study, we further characterized the SAR for the PAB series and synthesized compounds with antitubercular activity in the low nanomolar range, good cytotoxicity profiles, and intracellular activity against *M. tuberculosis*. We also identified the probable target of PAB compounds as QcrB, a component of the cytochrome *bc*₁ oxidase of the electron transport chain. This knowledge will enable the elucidation of the mechanism of

action for the strategic design of new compounds and combination therapies to treat *M. tuberculosis* infection.

RESULTS AND DISCUSSION

PAB Structure–Activity Relationship. The alkyl benzimidazoles were synthesized according to Scheme 1. Condensation of appropriate 1,2-diaminobenzene derivative with propionic acid yielded the benzimidazole intermediate (1) upon heating. Alkylation of the benzimidazole intermediate (1) was accomplished by reacting with dibromoalkane to form *N*-(bromoalkyl)-benzimidazole (2). This in turn was treated with the corresponding anilines, thiophenols, and phenols to yield the corresponding benzimidazole alkylamine, alkyl thioether, and alkyl ethers.

In our previous study, we observed that compounds with heteroatoms (O, S, and N) as part of the linker were tolerated, a linker length of three to four carbons was favored, and ethyl at the 2-position and methyl at the 6-position on the benzimidazole were the most favorable substituents on the core.² We first investigated aryl and heteroaryl thioethers for their activity against *M. tuberculosis*. Since compound 4 from our previous work showed good activity (Table 1),² we made analogues (6–18) to explore the SAR around the phenyl group of 4. In our

Received: July 25, 2017

Published: October 16, 2017

Scheme 1. Synthesis of Amine and Thioether Aryl, Hetero Aryl, and Cycloalkyl Benzimidazoles

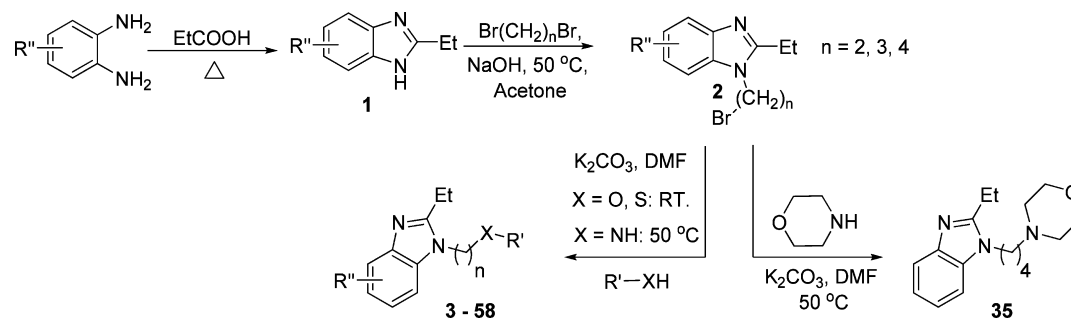


Table 1. Effect of Phenyl Replacements on Biological Activity

compd	name	R-group	MIC ₉₉ ^a (μM)	TC ₅₀ ^b (μM)	SI ^c
3 ^d	IDR-0333819	phenoxy	1.1 ± 0.4	21 ± 7.1	19
4 ^d	IDR-0341914	phenylthio	1.4 ± 0.3	31 ± 8.3	22
5 ^d	IDR-0351544	aniliny	0.47 ± 0.09	42 ± 7.8	89
6	IDR-0357446	4-methylphenyl	1.4 ± 0.56	19 ± 0.71	14
7	IDR-0458791	4-methoxyphenyl	4.8 ± 0.1	34 ± 12.8	7
8	IDR-0357447	2-naphthyl	4.1 ± 1.3	10 ± 0	2
9	IDR-0357452	2-quinoliny	18 ± 2.6	7 ± 0	0.4
10	IDR-0357451	2-quinoxaliny	10 ± 0	13 ± 0	1
11	IDR-0351547	6-ethoxy-2-benzothiazolyl	10 ± 2.1	12 ± 0.7	1
12	IDR-0351549	6-chloro-2-benzothiazolyl	6.0 ± 4.4	18 ± 2.2	3
13	IDR-0351556	2-benzimidazolyl	>20	18 ± 2.8	NC
14	IDR-0351555	N-methyl-2-benzimidazolyl	>20	16 ± 2.1	NC
15	IDR-0351552	2-thiazolyl	>20	>50	NC
16	IDR-0351550	5-methyl-2-thiazolyl	>20	>50	NC
17	IDR-0351557	N-methyl-5-tetrazolyl	>20	>50	NC
18	IDR-0351553	4-phenyl-2-thiazolyl	0.73	9.7	13

^aMIC₉₉ is the minimum concentration required to completely inhibit growth of *M. tuberculosis* in liquid culture. MICs of active compounds are the average of two independent experiments ± standard deviation. ^bTC₅₀ is the concentration required to inhibit growth of Vero cells by 50%. TC₅₀ is the average of two independent experiments ± standard deviation. ^cSelectivity index (SI) is TC₅₀/MIC. NC, not calculated. ^dData for compounds 3, 4, 5 are from compounds 6, 53, and 54, respectively, in ref 2.

previous studies on aryl ethers, we observed that the 4-methyl substitution improved both activity and selectivity. In the case of the aryl thioether analogues, 4-methyl substitution (6) did not show any improvement in activity, while 4-methoxy substitution (7) decreased activity by 4-fold (MIC = 4.8 μM). Replacement of the phenyl with biaryls or a heteroaryl ring, such as naphthalene (8), quinoline (9), quinazoline (10), benzothiazole (11 and 12) or benzimidazole (13 and 14) decreased activity while replacement with thiazole (15 and 16) or tetrazole (17) resulted in no activity (MIC > 20 μM). The 4-phenylthiazole (18) was the most active thioether analogue with an MIC of 0.73 μM. However, it was fairly cytotoxic to eukaryotic cells (TC₅₀ = 9.7 μM), despite the selectivity index (SI = 13) being similar to the earlier compounds.

In our previous SAR study, we observed that replacing the phenyl ether in compound 3 with 5-(4-chlorophenyl)oxadiazol-2-yl thioether as in 19 improved activity.² We attempted to improve this further by modifying the linker length (Table 2). Reduction of the linker length from four carbons to three (20) or two (21) was detrimental to the antitubercular activity; in the case of the propyl (20) linker, we observed a 39-fold reduction in

activity and further reduction of the linker to an ethyl (21) resulted in complete loss of activity. The addition of a weaker electron-releasing group such as the methyl group on the 6-position of the benzimidazole core (22) retained good potency (MIC = 0.085 μM). The combination of a 6-methyl on the benzimidazole core and a propyl linker (23) was slightly less active in comparison (MIC = 0.34 μM). Interestingly, replacing the 6-methyl with 6-methoxy, a strong electron-donating group, in compound 24, reduced activity by almost 10-fold (MIC = 2.5 μM).

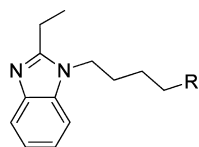
We next explored the influence of nitrogen as the heteroatom in the linker (Table 3). We synthesized compounds (25–35) to investigate the electronic and steric effects of different aromatic substituents on the terminal aniline. The addition of the electron donating groups methyl (25) or methoxy (26) made no improvement in activity, although the methyl analogue was slightly more active. A trifluoromethyl substituent at the meta position (27) had a comparable MIC to compound 5. However, the cytotoxicity was significantly worse than that of 5 and the selectivity was 8-fold lower. The 3,5-dimethoxy (28) lost activity, whereas the 3-halo and 4-methyl substituted anilines (29,30) showed comparable activity to that of 5. The substituents

Table 2. Effect of N-Alkyl Chain Length and Benzo Substitution on Biological Activity

Compound	Name	Structure	MIC ₉₉ ^a (μ M)	TC ₅₀ ^b (μ M)	SI ^c
19 ^d	IDR-0351551		0.10 \pm 0.07	22 \pm 9.2	220
20	IDR-0390229		3.9 \pm 0.21	21 \pm 2.1	5
21	IDR-0351587		>20	35 \pm 2.8	NC
22	IDR-0390228		0.085 \pm 0.007	18 \pm 0	212
23	IDR-0390226		0.34 \pm 0.19	21 \pm 2.8	62
24	IDR-0458783		2.5 \pm 0.2	49 \pm 2.6	20

^aMIC₉₉ is the minimum concentration required to completely inhibit growth of *M. tuberculosis* in liquid culture. MICs of active compounds are the average of two independent experiments \pm standard deviation. ^bTC₅₀ is the concentration required to inhibit growth of Vero cells by 50%. TC₅₀ is the average of two independent experiments \pm standard deviation. ^cSelectivity index (SI) is TC₅₀/MIC. NC, not calculated. ^dData for compound 19 is from compound 68 in ref 2.

Table 3. Effect of Aniliny Substitution on the Biological Activity



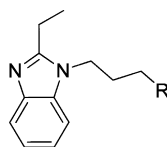
cmpd	name	R	MIC ₉₉ ^a (μ M)	TC ₅₀ ^b (μ M)	SI ^c
5 ^d	IDR-0351544	aniliny	0.47 \pm 0.09	42 \pm 7.8	89
25	IDR-0357431	4-methylaniliny	0.50 \pm 0.1	39 \pm 1.4	78
26	IDR-0458786	4-methoxyaniliny	1.4 \pm 1.1	>100	>71
27	IDR-0351602	3-trifluoromethylaniliny	1.1 \pm 0.9	12 \pm 2.6	11
28	IDR-0351605	3,5-dimethoxyaniliny	4.4 \pm 1.5	21 \pm 4.6	5
29	IDR-0351599	3-bromo-4-methylaniliny	0.45 \pm 0.07	17 \pm 0	38
30	IDR-0458790	3-chloro-4-methylaniliny	0.35 \pm 0.07	53 \pm 27.0	151
31	IDR-0351600	3-benzyloxyaniliny	0.60 \pm 0	14 \pm 3.8	23
32	IDR-0351601	4-(2-pyridyl)aniliny	0.80 \pm 0.7	22 \pm 2.1	28
33	IDR-0351606	3-(2-pyridyl)aniliny	3.7 \pm 0.8	19 \pm 3.8	5
34	IDR-0351603	N-benzylamino	>20	>50	NC
35	IDR-0357457	N-morpholiny	>20	>100	NC

^aMIC₉₉ is the minimum concentration required to completely inhibit growth of *M. tuberculosis* in liquid culture. MICs of active compounds are the average of two independent experiments \pm standard deviation. ^bTC₅₀ is the concentration required to inhibit growth of Vero cells by 50%. TC₅₀ is the average of two independent experiments \pm standard deviation. ^cSelectivity index (SI) is TC₅₀/MIC. NC, not calculated. ^dData for compound 5 is from compound 54 in ref 2.

3-benzyloxy (31) and 4-pyridyl (32) showed similar activity to that of 5, but the 3-pyridyl (33) was much less active (MIC = 3.7 μ M). Moving from the aniline (5) to benzylamine

(34) was detrimental to the antitubercular activity. Replacing the terminal aniline with a morpholino group also resulted in loss of activity (35).

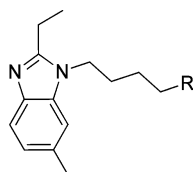
Table 4. Effect of Phenyl Ring Substitutions on Biological Activity



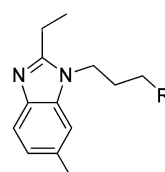
compd	name	R	MIC ₉₉ ^a (μM)	TC ₅₀ ^b (μM)	SI ^c
36 ^d	IDR-0257287	phenoxy	5.2 ± 1.9	>50	>10
37	IDR-0357449	anilinyll	0.45 ± 0.2	29 ± 4.9	64
38	IDR-0357444	4-methylphenoxy	1.6 ± 0.2	14 ± 0.7	9
39	IDR-0357448	4-methylphenylthio	4.5 ± 0.8	24 ± 2.8	5
40	IDR-0357450	4-methylanilinyll	0.12 ± 0.07	31 ± 3.5	258
41	IDR-0357442	3,4-dimethylanilinyll	0.65 ± 0.4	>100	>154
42	IDR-0357458	3-bromo-4-methylanilinyll	0.04 ± 0	11 ± 0.7	275
43	IDR-0357443	3-chloro-4-methylphenoxy	0.55 ± 0.35	16 ± 0	29

^aMIC₉₉ is the minimum concentration required to completely inhibit growth of *M. tuberculosis* in liquid culture. MICs of active compounds are the average of two independent experiments ± standard deviation. ^bTC₅₀ is the concentration required to inhibit growth of Vero cells by 50%. TC₅₀ is the average of two independent experiments ± standard deviation. ^cSelectivity index (SI) is TC₅₀/MIC. ^dData for compound 36 is from compound 5 in ref 2.

Table 5. Effect of Phenyl SAR on Biological Activity



44 - 53



54 - 58

compd	name	R	MIC ₉₉ ^a (μM)	TC ₅₀ ^b (μM)	SI ^c
44 ^d	IDR-0357433	anilinyll	0.32 ± 0.09	22 ± 0.7	69
45	IDR-0341934	phenylthio	0.22 ± 0.02	9.5 ± 0.7	43
46 ^d	IDR-0341930	phenoxy	0.27 ± 0.09	18 ± 2.5	67
47	IDR-0458750	4-methoxyphenoxy	0.4 ± 0.1	27 ± 6.4	68
48	IDR-0458784	4-methoxyanilinyll	0.65 ± 0.07	14 ± 2.1	22
49	IDR-0458789	4-methoxyphenylthio	2.3 ± 0.4	20 ± 2.1	9
50	IDR-0357439	3-chloroanilinyll	2.1 ± 0.9	16 ± 9.0	8
51	IDR-0357436	3-trifluoromethylanilinyll	0.55 ± 0.4	5.7 ± 1.5	10
52	IDR-0357435	3-benzyloxyanilinyll	1.8 ± 0.76	18 ± 0.7	10
53	IDR-0357445	4-chlorophenylthio	2.6 ± 0.6	16 ± 1.4	6
54	IDR-0578347	anilinyll	0.056 ± 0.020	>50	>893
55	IDR-0390234	4-methylanilinyll	0.066 ± 0.018	31 ± 0.7	470
56	IDR-0458788	4-methoxyanilinyll	0.35 ± 0.2	91 ± 12.3	260
57	IDR-0390235	2,4-dimethylanilinyll	0.070 ± 0.03	14 ± 0.7	200
58	IDR-0458745	4-methoxyphenylthio	0.88 ± 0.2	33 ± 11	38

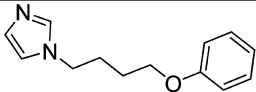
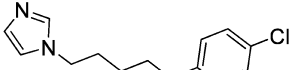
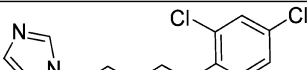
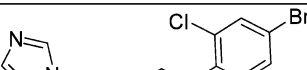
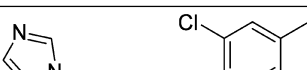

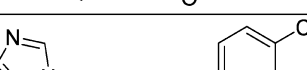

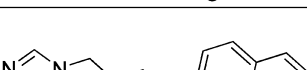
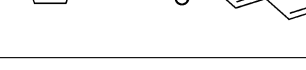
^aMIC₉₉ is the minimum concentration required to completely inhibit growth of *M. tuberculosis* in liquid culture. MICs of active compounds are the average of two independent experiments ± standard deviation. ^bTC₅₀ is the concentration required to inhibit growth of Vero cells by 50%. TC₅₀ is the average of two independent experiments ± standard deviation. ^cSelectivity index (SI) is TC₅₀/MIC. ^dData for compounds 44 and 46 are from compounds 55 and 34, respectively, in ref 2.

4-Bromo-*N*-(3-(2-ethyl-6-methyl-1*H*-benzo[d]imidazol-1-yl)propyl)-3-methylaniline, compound 62 from Chandrasekera et al.² was the most potent and selective in our previous study.² This compound contained only three carbons in the lipophilic linker. We prepared additional analogues 36–43 to understand the SAR surrounding the phenyl region of three-carbon tethered benzimidazole molecules. The phenyl ether analogue (36) had good activity (MIC = 5.2 μM), but the corresponding aniline analogue (37) was 10-fold more active. Electron withdrawing 4-methyl substitution on phenyl ether (38) or thioether (39) analogues improved activity. The aniline analogue with a 4-methyl group (40) also showed good activity (MIC = 0.12 μM) and

selectivity (SI = 258). In comparison, double substitution to the more electron-rich 3,4-dimethylaniline analogue (41) slightly reduced activity but a combination of electron-withdrawing group at 3-position and methyl at 4-position (42) resulted in the most potent of all the alkyl benzimidazoles (Table 4) with a MIC of 0.040 μM and good selectivity (SI = 275). Interestingly, a 3-chlorine substitution instead of the 3-bromine substitution was ~10-fold less active (MIC = 0.55 μM).

We then investigated the effect of 6-methyl substitution on the benzimidazole core bearing a 4-carbon tether to various aromatics (Table 5). The aniline (44), phenyl thioether (45), and phenyl ether (46) had comparable activities. 4-Methoxy

Table 6. SAR of Phenoxy Alkyl Imidazole Analogues with Varying Linker Length

Compound	Name		MIC ₉₉ ^a (μ M)	TC ₅₀ ^b (μ M)	SI ^c
59	IDR-0122293		> 20	> 50	NC
60	IDR-0124213		> 20	ND	NC
61	IDR-0124480		20	16 \pm 0	0.8
62	IDR-0257359		11 \pm 2.3	35 \pm 11	3
63	IDR-0262047		20	21	1
64	IDR-0262049		> 20	ND	NC
65	IDR-0262053		20	40	2
66	IDR-0155469		9.9 \pm 1.7	19 \pm 9.3	2
67	IDR-0123367		> 20	89 \pm 2.5	NC
68	IDR-0168354		8.6 \pm 0.9	15 \pm 0.3	2

^aMIC₉₉ is the minimum concentration required to completely inhibit growth of *M. tuberculosis* in liquid culture. MICs of active compounds are the average of two independent experiments \pm standard deviation. ^bTC₅₀ is the concentration required to inhibit growth of Vero cells by 50%. TC₅₀ is the average of two independent experiments \pm standard deviation. ^cSelectivity index (SI) is TC₅₀/MIC. ND, not determined. NC, not calculated.

substitution on the phenyl ether (47) or aniline (48) had minimal effect on activity, but this substitution resulted in a 10-fold shift in the activity of a corresponding phenyl thioether (49). Both 3-chloroaniline (50) and 4-chlorophenyl thioether (53) were less active, but a 3-trifluoromethyl substitution on aniline (51) retained all activity of parent compound 44. We also tested 3-benzyloxy aniline (52) with good activity.

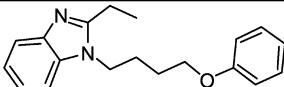
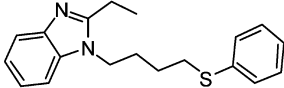
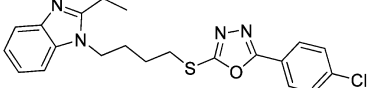
We finally probed the effect of combination of the optimized residues, namely, the three-carbon linker and a 6-methyl substitution on the benzimidazole core (54–58). Four compounds had a selectivity index of >200 (54, 55, 56, and 57) (Table 5). The aniline analogues 54, 55, and 57 had the best activities with comparable MICs of 0.061 μ M, 0.067 μ M, and 0.070 μ M, respectively. While 54 had no cytotoxicity at 50 μ M, the addition of one (55) or two (56) methyl groups on the phenyl ring caused a stepwise increase in cytotoxicity toward eukaryotic cells, thus reducing the selectivity index from >819 (54) to 470 and 200 for

55 and 57, respectively (Table 5). The methoxy analogue (56) was 5-fold less active (Table 5).

Several phenoxy alkyl imidazoles 59–68 were evaluated to study the importance of the benzimidazole core for the anti-tubercular activity of PAB (Table 6). Many of the compounds lost activity (59, 60, 64, and 67), while others maintained only moderate activity compared to benzimidazole variants (61, 62, 63, 65, 66, and 68). These data show the benzene of the benzimidazole core is not strictly required; several imidazole variants maintain moderate activity against *M. tuberculosis*. However, the benzene ring does appear to confer optimal antitubercular activity to PAB compounds.

PAB Compounds Target QcrB. To identify the target of PAB compounds, we isolated resistant mutants against three different PABs. Of the seven confirmed mutants, five contained mutations in *qcrB*, the Cytochrome *b* subunit of the cytochrome *bc*₁ oxidase (Rv2196), while two of the three mutants raised

Table 7. Resistant Mutant Strains Isolated against PAB Compounds

Compound	Name	Structure	Gene	Mutation
3	IDR-0333819		<i>qcrB</i>	A179P
4	IDR-0341914		Rv1339	V90M
			<i>qcrB</i>	A179P
			Rv1339	Y94C
19	IDR-0351551		<i>qcrB</i>	M342T
			<i>qcrB</i>	W312C
			<i>qcrB</i>	W312G

against compound 4 contained mutations in Rv1339, a gene of unknown function (Table 7).

We confirmed targeting of QcrB by PABs by testing the MIC of 30 active compounds against LP-0351551-RM1 (QcrB_{M342T}), one of the isolated resistant mutants. All compounds tested showed a minimum 5-fold shift in MIC compared to the parental strain with 78% of the compounds having at least a 10-fold higher MIC (Table 8). Most compounds had similar MICs against LP-0341914-RM5 (Rv1339_{V90M}) as against the wild-type strain (Table 9). Six compounds had 5-fold shifts in MIC against the Rv1339_{V90M} mutant, but in all cases the observed resistance shift was significantly smaller than those observed when the same compounds were tested against the QcrB_{M342T} mutant (Tables 8 and 9). Together, these data indicate the Rv1339 gene product is unlikely to play a major role in resistance to the PAB series and implicates QcrB as the target of PAB compounds.

Structurally, the benzene of the benzimidazole core of the PAB series is not required for antituberculosis activity, as some compounds with just an imidazole ring (PAB-II) still have moderate activity against *M. tuberculosis* (Table 6). However, the PAB-II compounds appear to have a different target or mode of action, since the QcrB_{M342T} mutant strain was not resistant to this set (Table 10). This argues that while the benzene ring of the core may not be strictly required for whole-cell activity, this ring may be responsible for targeting of QcrB specifically. It would be interesting to elucidate the target of PAB-II compounds to determine their mechanism of action.

As a key component of the mycobacterial electron-transport chain, QcrB receives electrons from menaquinol and serves as a pump shuttling protons into the periplasmic space, thereby establishing the proton gradient required for ATP production.³ Over the past few years, the cytochrome *bc*₁ oxidase has been discovered to be the target of novel drugs against numerous infectious diseases including malaria and *Leishmania* parasites, as well as multiple classes of compounds active against *M. tuberculosis*, including the drug Q203, an imidazopyridine amide currently in clinical trials.^{4–8} Two of the resistance mutations found in our study cause amino acid changes at position 312 of QcrB, which sits in the same pocket as the resistant mutant at position 313 found for Q203.⁸ This suggests the PAB compounds may be binding in the same location and have a similar mechanism of action as Q203. To test this, we examined cross-resistance of PAB compounds to a strain of *M. tuberculosis* containing the same mutation found in Q203-resistant isolates (QcrB_{T313I}). PAB compounds were highly resistant to the QcrB_{T313I} variant; the MIC₉₀ for PAB compounds ranged from 13-fold up to 200-fold higher compared to the wild-type strain

Table 8. Cross-Resistance of QcrB_{M342T} Mutant Strain to PAB Compounds

cmpd	name	WT MIC ₉₀ ^a (μM)	QcrB _{M342T} MIC ₉₀ ^a (μM)	fold-change
3	IDR-0333819	16	>100	>6.3
4	IDR-0341914	20	>100	>5.0
6	IDR-0357446	8.3	>100	>12
18	IDR-0351553	5.7	>100	>18
19	IDR-0351551	0.15	47	313
20	IDR-0390229	8	>100	>13
22	IDR-0390228	6	>100	>17
26	IDR-0458786	6.9	>100	>15
28	IDR-0351605	1	5	5.0
30	IDR-0458790	1.6	93	58
32	IDR-0351601	0.55	22	40
37	IDR-0357449	2.7	>100	>37
38	IDR-0357444	7.6	>100	>13
41	IDR-0357442	3.1	35	11
43	IDR-0357443	3.8	44	12
44	IDR-0357433	0.21	8.6	41
46	IDR-0341930	1.3	73	56
49	IDR-0458789	9.4	98	10
52	IDR-0357435	6.7	70	10
53	IDR-0357445	16	>100	>6.3
54	IDR-0578347	0.10	4.1	41
57	IDR-0390235	1	6.2	6.2
58	IDR-0458745	4.6	98	21
69 ^b	IDR-0341919	0.92	16	17
70 ^b	IDR-0341920	5	>100	>20
71 ^b	IDR-0341931	7.7	87	11
72 ^b	IDR-0341936	14	>100	>7.1
73 ^b	IDR-0341926	3.5	31	8.9
74 ^b	IDR-0341921	13	>100	>7.7
75 ^b	IDR-0357430	0.88	48	55
76 ^b	IDR-0390233	0.66	>100	>152

^aMIC₉₀ is the concentration required to inhibit growth of *M. tuberculosis* by 90%. LP-0351551-RM1 is QcrB_{M342T}. ^bCompounds 69–76 are compounds 13, 15, 22, 23, 29, 30, 56, and 62, respectively, in ref 2.

(Table 11). The fold-change in MIC against QcrB_{T313I} was larger than that for QcrB_{M342T} for every compound tested except IDR-0351551, the compound against which QcrB_{M342T} was raised. When Q203 was tested against QcrB_{W312C}, the MIC was greater than 100 nM compared to just 2.8 nM for H37Rv-LP. Together, these data suggest an overlapping binding site between Q203 and PAB compounds.

To provide further evidence supporting QcrB as the target of PAB compounds, we performed initial mechanistic studies

Table 9. Cross-Resistance of *M. tuberculosis* Rv1339_{V90M} Mutant Strain to PAB Compounds

compd	name	WT MIC ₉₀ ^a (μ M)	Rv1339 _{V90M} MIC ₉₀ ^a (μ M)	fold-change
3	IDR-0333819	16	6.2	0.4
18	IDR-0351553	5.7	9.6	1.7
19	IDR-0351551	0.15	1.5	10
20	IDR-0390229	8	10	1.3
22	IDR-0390228	6	2.9	0.5
26	IDR-0458786	6.9	3	0.4
30	IDR-0458790	1.6	0.77	0.5
32	IDR-0351601	0.55	6.3	12
37	IDR-0357449	2.7	1.8	0.7
38	IDR-0357444	7.6	6.9	0.9
46	IDR-0341930	1.3	1.7	1.3
49	IDR-0458789	9.4	10	1.1
52	IDR-0357435	6.7	3.5	0.5
53	IDR-0357445	16	12	0.8
58	IDR-0458745	4.6	6.8	1.5
69 ^b	IDR-0341919	0.92	6.2	6.7
70 ^b	IDR-0341920	5	2.3	0.5
71 ^b	IDR-0341931	7.7	5.9	0.8
72 ^b	IDR-0341936	14	13	0.9
73 ^b	IDR-0341926	3.5	2.1	0.6
74 ^b	IDR-0341921	13	7.8	0.6
75 ^b	IDR-0357430	0.88	0.74	0.8
76 ^b	IDR-0390233	0.66	0.62	0.9

^aMIC₉₀ is the concentration required to inhibit growth of *M. tuberculosis* by 90%. ^bCompounds 69, 70, 71, 72, 73, 74, 75, 76 are compounds 13, 15, 22, 23, 29, 30, 56, and 62, respectively, from ref 2.

Table 10. Cross-Resistance of *M. tuberculosis* QcrB_{M342T} Mutant Strain to PAB-II Compounds

compd	name	WT MIC ₉₀ ^a (μ M)	QcrB _{M342T} MIC ₉₀ ^a (μ M)	fold-change
63	IDR-0262047	34	47	1.4
66	IDR-0155469	8.1	8.7	1.1
68	IDR-0168354	9.4	10	1.1

^aMIC₉₀ is the concentration required to inhibit growth of *M. tuberculosis* by 90%.

Table 11. Cross-Resistance of QcrB_{T313I} Mutant Strain to PAB Compounds

compd	name	WT MIC ₉₀ ^a (μ M)	QcrB _{T313I} MIC ₉₀ ^a (μ M)	fold-change
19	IDR-0351551	0.39	63	161
28	IDR-0351605	2.4	>100	>41
32	IDR-0351601	1.9	>100	>52
44	IDR-0357433	0.45	89	198
52	IDR-0357435	2.2	>100	>45
54	IDR-0578347	0.10	8.7	87
69 ^b	IDR-0341919	0.87	61	70
71 ^b	IDR-0341931	7.7	>100	>13
77 ^b	Q203	0.0088	1.7	193

^aMIC₉₀ is the concentration required to inhibit growth of *M. tuberculosis* by 90%. ^bCompounds 69 and 71 are compounds 13 and 22, respectively, in ref 2. Compound 77 is from ref 8.

surrounding QcrB. Inhibition of QcrB leads to reduced proton pumping across the bacterial membrane. An inability to pump protons disrupts ATP production and increases the concentration of protons within the cell, thus lowering intrabacterial pH (pHIB). As would be expected following QcrB inhibition, PAB

compounds caused ATP depletion over a 24 h time-period (Figure 1A) and significantly decreased pHIB; all PAB compounds caused a reduction in pHIB to at least 6.7 with 8/16 compounds dropping the pHIB below 6.5, similar to that seen with the ionophore monensin (Figure 1B). The one PAB-II compound tested showed no activity in this assay, consistent with the conclusion QcrB is not its target. Together with the resistant mutant isolation, these data strongly support QcrB as the target for PAB compounds and suggest potential mechanisms for compound activity.

Previous studies identified PAB compounds as bacteriostatic against actively growing *M. tuberculosis*, while bactericidal against nutrient-starved bacteria.² We tested this for two compounds, including one of our most potent compounds, IDR-0578347 (S4). Both compounds had similar activity; when tested at 10 \times their respective MICs, the compounds inhibited growth of *M. tuberculosis* grown aerobically but displayed bactericidal activity only in the context of nutrient starvation (Figure 2A,B). One possible explanation for the differential activity stems from the elucidation of QcrB as the target. Under replicating conditions individual bacteria contain large amounts of ATP necessary to support growth and division of bacterial cells. Under starvation conditions ATP is still required to maintain basal cellular processes, but the amount of ATP/cell is much reduced.⁹ It is possible ATP depletion mediated by PAB compounds during replicative growth is only enough to inhibit growth and force the bacteria into a nonreplicative state, while under starvation conditions any reduction from the basal amount of ATP being produced is enough to cause bacterial cell death. This hypothesis still needs to be tested experimentally.

The number of series of compounds that target QcrB has led to an intriguing debate within the field. On one hand, the number of times this target has been identified highlights the importance of the cytochrome *bc*₁ complex and ETC to mycobacterial survival.³ However, there has been concern as to the promiscuity of the target, the similarity to the human electron transport chain, and the ability of *M. tuberculosis* to adapt by using the *bd* oxidase as an alternative electron acceptor under oxygen-limited conditions.^{10,11} Recent work used the adaptability of *M. tuberculosis* against itself by using combination therapy targeting the ETC.¹² On the basis of our results, it is possible the PAB series could similarly be used in combination with other electron-transport inhibitors. These studies are currently underway.

As for the potential consequence of targeting a component of the electron transport chain, our previously published data suggests the inhibitors described herein are specific to *M. tuberculosis*, as PAB compounds do not inhibit growth of several other bacteria, including *M. smegmatis*.² In fact, when tested against *M. tuberculosis* in a high-content analysis of *M. tuberculosis* macrophage infection, PAB compounds showed exquisite sensitivity toward bacterial cells with MICs against *M. tuberculosis* inside macrophages similar to those found in liquid broth and selectivity indexes ranging from 19 to nearly 2000 (Table 12). Several compounds even appeared to be slightly more active inside macrophages than in liquid culture. Together, these data show the penetration of these compounds into eukaryotic cells, while highlighting the safety of the PAB compounds, offering a promising therapeutic window that would allow for treatment of infection while minimizing host cell toxicity.

CONCLUSION

This work investigated a range of possible amine and thioether linkages as a strategy to identify improved alkyl benzimidazole

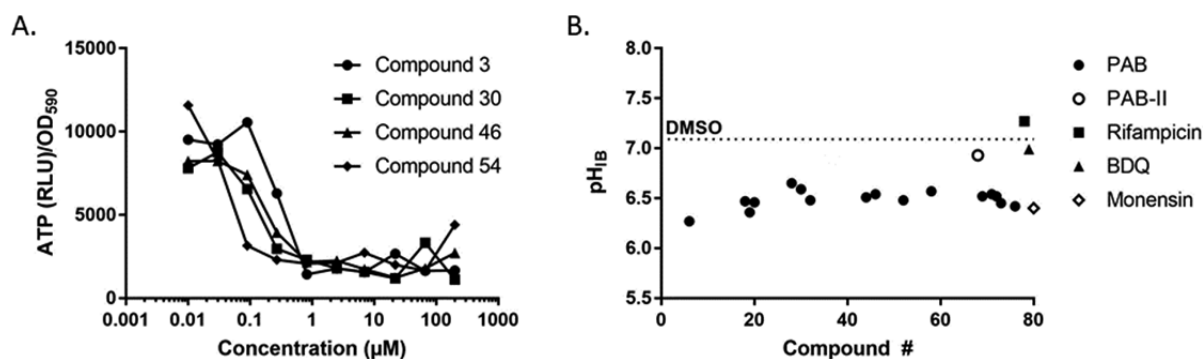


Figure 1. PAB compounds deplete ATP and disrupt pH homeostasis. (A) ATP levels of *M. tuberculosis* H37Rv-LP treated with compounds at the indicated concentrations for 24 h. ATP levels are calculated as relative luminescence units divided by optical density to account for potential differences in bacterial growth. (B) Intracellular pH of *M. tuberculosis* treated with PAB or reference compounds for 48 h. Compound no. refers to compounds as listed in tables above. Data are representative of at least two independent experiments.

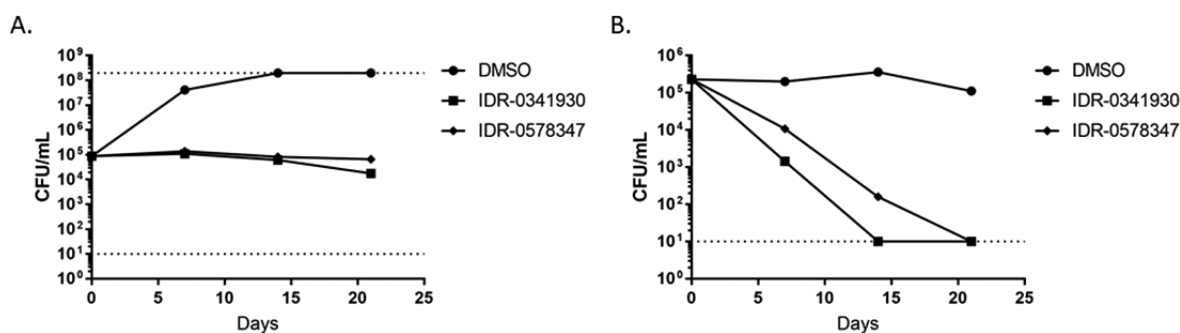


Figure 2. PAB compounds are bactericidal against nutrient-starved *M. tuberculosis*. PAB compounds at 10 \times their respective MICs were added to *M. tuberculosis* grown aerobically (A) or after nutrient starvation in PBS 0.05% Tyloxapol for 2 weeks (B). Serial dilutions were performed and plated for CFUs at the indicated times. Data are representative of at least two independent experiments.

Table 12. Activity of PAB Compounds against Intracellular *M. tuberculosis*

cmpd	ID	intracellular IC ₅₀ ^a (μ M)	intracellular IC ₉₀ ^b (μ M)	TC ₅₀ (μ M) ^c	SI ^d
18	IDR-0351553	0.27 \pm 0.05	0.86 \pm 0.14	17 \pm 3.5	19
44	IDR-0357433	0.040 \pm 0.002	0.15 \pm 0.04	49 \pm 14.9	325
46	IDR-0341930	0.070 \pm 0.006	0.29 \pm 0.06	28 \pm 0.5	95
54	IDR-0578347	0.0073 \pm 0.0009	0.028 \pm 0.001	>50	>1785
73	IDR-0341926	0.093 \pm 0.01	0.30 \pm 0.05	26 \pm 3.2	85
77 ^e	IDR-0341939	0.48 \pm 0.03	1.3 \pm 0.16	38 \pm 5.6	29

^aIntracellular IC₅₀ is the concentration required to inhibit growth of *M. tuberculosis* inside macrophages by 50%. ^bIntracellular IC₉₀ is the concentration required to inhibit growth of *M. tuberculosis* inside macrophages by 90%. ^cTC₅₀ is the concentration required to inhibit growth of RAW cells by 50%. Data are the average of four experiments \pm standard deviation. ^dSelectivity index (SI) = TC₅₀/IC₉₀. ^eCompound 77 is compound 67 from ref 2.

molecules. Several compounds showed good potency and selectivity as well as activity against intracellular bacteria. The key determinants for optimal antimycobacterial activity of the compounds are methyl groups in both the C-6 position of the benzimidazole and the para position of the terminal phenyl ring, a three or four carbon atom linker, a nitrogen as the heteroatom on the alkyl chain, and a benzimidazole as the core moiety. The PAB compounds appear to target QcrB, a component of the *M. tuberculosis* electron transport chain, suggesting they could be useful in combination therapy with other electron-transport chain inhibitors.

METHODS

Bacterial Strains and Growth Conditions. *M. tuberculosis* H37Rv (London Pride) (ATCC 25618)¹³ was used for all work. *M. tuberculosis* strains were grown in Middlebrook 7H9 medium containing 10% v/v OADC (oleic acid, albumin, dextrose, catalase) supplement (Becton Dickinson) and 0.05% w/v Tween 80 (7H9-Tw-OADC) under aerobic conditions.

Determination of Minimum Inhibitory Concentration (MIC). MICs were performed as previously described;¹⁴ briefly MIC_{99s} were determined against *M. tuberculosis* H37Rv-LP constitutively expressing codon-optimized mCherry grown in 7H9-Tw-OADC under aerobic conditions. Bacterial growth was measured by OD₅₉₀ after 5 days of incubation at 37 °C. MIC₉₉ was defined as the minimum concentration required for >99% growth inhibition using the Gompertz model. MIC₉₀ values were determined against *M. tuberculosis* H37Rv-LP or indicated mutants under the same growth conditions. MIC₉₀ is defined as the concentration of compound required to inhibit growth of *M. tuberculosis* by 90% and was determined from the Levenberg–Marquardt least-squares plot.¹⁵

Cytotoxicity Assay. Cytotoxicity was determined against the Vero African green monkey kidney cell line (ATCC CCL-81). Cells were cultured in Dulbecco's Modified Eagle Medium (DMEM), High Glucose, GlutaMAX (Invitrogen), 10% v/v FBS (Fetal Bovine Serum), and 1 \times of Penicillin-Streptomycin

Solution (100 units/mL of penicillin, 100 μ g/mL of streptomycin). Cells were plated into 96-well plates and allowed to adhere for 24 h before exposure to compounds for 48 h. CellTiter-Glo Reagent (Promega) was added to 96-well plates and relative luminescent units (RLU) were measured. Inhibition curves were fitted using the Levenberg–Marquardt algorithm. Toxic concentration (TC_{50}) was defined as the concentration of compound that gave 50% inhibition of growth.

Resistant Mutant Isolation. *M. tuberculosis* H37Rv-LP was plated on 7H10-OADC plates containing 5 \times or 10 \times MIC of three PAB compounds **3**, **4**, and **19** (Compounds **6**, **53**, and **68** from ²). Resistant clones raised against compounds **4** and **19** were isolated, confirmed, and whole genome-sequenced as previously described.¹⁶ The resistant clone raised against compound **3** was isolated and confirmed by sequencing.

ATP Depletion Assay. *M. tuberculosis* H37Rv-LP was grown in duplicate at 37 °C for 24 h in the presence of 3-fold dilutions of PAB compounds starting at 200 μ M. ATP levels were measured using the BacTiter-Glo assay kit (Promega) according to the manufacturer's instructions. OD₅₉₀ of the duplicate plate was measured using a Synergy H4 plate reader (BioTek). ATP/OD was calculated by dividing relative fluorescent units from the BacTiter-Glo plate by OD₅₉₀ readings.

pH Homostasis Assay. *M. tuberculosis* H37Rv-LP containing a pH-sensitive ratiometric GFP reporter¹⁷ was added to compounds at 100 μ M final concentration in phosphocitrate buffer at pH 4.5. After 48 h fluorescence was read and intrabacterial pH was determined based on the ratio between Ex396/Em510 and Ex475/Em510.

Determination of Compound Kill Kinetics. *M. tuberculosis* H37Rv-LP was inoculated into 7H9-Tw-OADC at 1 \times 10⁵ CFU/mL in the presence of 10 \times the respective MIC of either compound **46** or **54** or a DMSO control (final DMSO concentration of 2%). For starvation experiments, H37Rv-LP was washed and resuspended in phosphate-buffered saline (PBS) + 0.05% Tyloxapol at 1 \times 10⁵ CFU/mL for 2 weeks prior to compound addition. Serial dilutions were performed at the indicated times and bacteria were plated on 7H10-OADC agar plates for CFU enumeration.

Intracellular Activity. Activity against intracellular bacteria was tested as described.¹⁸ In brief, RAW 264.7 cells were batch-infected overnight in RPMI-1640, 10% v/v FBS, 2 mM Glutagro, 1 mM sodium pyruvate medium with *M. tuberculosis* DREAM8 (an H37Rv variant constitutively expressing dsRED)¹⁹ at a multiplicity of infection of 1. Cells were harvested, washed twice, and seeded into 384-well assay plates at 3.3 \times 10³ cells per well. Infected cells were exposed to compounds for 72 h, and Macrophage nuclei were stained with SYBR Green I dye and imaged on an ImageXpress Micro with a 4 \times objective using a FITC filter set. *M. tuberculosis* were imaged using a Texas Red filter set. Images were analyzed by setting a lower bound for pixel intensity for each channel to define nuclei and bacteria above the background. The integrated intensity of each channel above this threshold was determined. Raw data were normalized to the average integrated control wells. Growth inhibition curves were fitted using the Levenberg–Marquardt algorithm. The IC₅₀ and IC₉₀ were defined as the compound concentration that produced 50% or 90% of the growth inhibitory response, respectively, for each readout.

■ COMPOUND SYNTHESIS

Compounds **59**–**68** were purchased from Chembridge.

General Methods. ¹H NMR (300 MHz) spectra were recorded on a Bruker Biospin NMR spectrometer. Reactions

were monitored using thin-layer chromatography (TLC) using Whatman silica gel 60 Å plates with a fluorescent indicator and visualized using a UV lamp (254 nm). Flash chromatography was performed on Grace with GraceResolv Normal Phase disposable silica columns. High-performance liquid chromatography (HPLC) was performed on a Gilson 322 HPLC pump with a Gilson UV/vis-155 detector and a Phenomenex Gemini C18 column (10 μ m, 250 mm \times 10 mm). The purity of all final products was >95% as determined by HPLC analysis conducted on an Agilent 1100 HPLC-MS system (Phenomenex Gemini C18 column, 5 μ m, 3 mm \times 50 mm, 0.45 mL/min, UV 254 nm, room temperature) with gradient elution (5–95% acetonitrile in water over 8 min with all solvents containing 0.05% formic acid). Liquid chromatography–electrospray ionization mass spectrometry (LC–MS/ESI–MS) were acquired on an Agilent LC/MSD-SL with a 1100 HPLC and G1956B mass spectrometer with a Phenomenex Gemini 5 μ m C18 110 Å 50 mm \times 3 mm column. High-resolution mass spectra (HRMS–ESI) were acquired by the Mass Spectrometry Laboratory at the University of Michigan on an Agilent Q-TOF HPLC–MS.

General Procedure for Synthesis of 1H-Benzo[d]imidazole Intermediates (1). 1H-Benzo[d]imidazole intermediates were synthesized according to the reported procedure.²

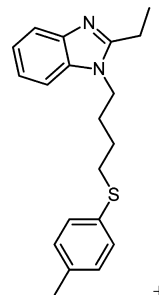
General Procedure for Synthesis of 1-(2-Bromoalkyl)-1H-benzo[d]imidazole Intermediates (2). 1-(2-Bromoalkyl)-1H-benzo[d]imidazole intermediates were synthesized according to the reported procedure.²

For the synthesis of 1-(2-bromoalkyl)-6-methyl-1H-benzo[d]imidazole intermediates, two isomers were formed and separated chromatographically. Both isomers were characterized by ¹H NMR and the desired intermediate was carried forward.²

General Procedure for Preparation of Compounds 6–18, 25–35, 37–43, 45, and 47–58. To a solution of benzimidazole in dimethylformamide were added 5 mol equiv of potassium carbonate and 2 mol equiv of the appropriate alcohol (or thiol). The reaction was stirred overnight at room temperature or until disappearance of the starting material monitored by TLC. Heating of the reaction to 50 °C was necessary to prepare the amine analogues using the same protocol. The reaction mixture was washed with water and extracted with ethyl acetate. The organics were dried with anhydrous sodium sulfate and concentrated *in vacuo*. The crude mixture was purified by column chromatography.

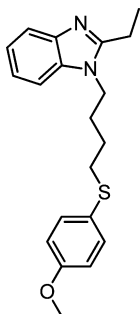
General Procedure for Preparation of Compounds 20–24. To a solution of benzimidazole in dimethylformamide were added 5 mol equiv of potassium carbonate and 2 mol equiv of 5-(4-chlorophenyl)-1,3,4-oxadiazole-2-thiol. The reaction was stirred overnight at room temperature or until all of the starting material disappeared. The reaction mixture was washed with water and extracted with ethyl acetate. The organics were dried with anhydrous sodium sulfate and concentrated *in vacuo*. The crude mixture was purified by column chromatography.

2-Ethyl-1-(4-(*p*-tolylthio)butyl)-1H-benzo[d]imidazole.



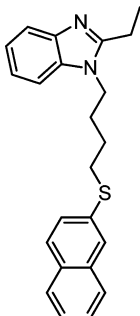
Compound 6: Yield = 80%. ^1H NMR (300 MHz, chloroform-*d*) δ 1.46 (t, J = 7.5 Hz, 3H), 1.55–1.78 (m, 2H), 1.78–2.05 (m, 2H), 2.32 (s, 3H), 2.69–2.99 (m, 4H), 4.07 (t, J = 7.4 Hz, 2H), 7.06–7.73 (m, 8H). LCMS-ESI ($M + H$) $^+$: 325.2. HRMS (ESI): calcd for $\text{C}_{20}\text{H}_{25}\text{N}_2\text{S}^+$, 325.1733; found, 325.1738.

2-Ethyl-1-(4-((4-methoxyphenyl)thio)butyl)-1H-benzo[d]imidazole.



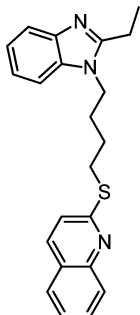
Compound 7: Yield = 74%. ^1H NMR (300 MHz, Chloroform-*d*) δ 1.48 (t, J = 7.5 Hz, 3H), 1.54–1.72 (m, 2H), 1.82–2.08 (m, 2H), 2.70–2.98 (m, 4H), 3.81 (s, 3H), 4.10 (t, J = 7.3 Hz, 2H), 6.82 (d, J = 8.6 Hz, 2H), 7.17–7.37 (m, 5H), 7.56–7.87 (m, 1H). LCMS-ESI ($M + H$) $^+$: 341.0. HRMS (ESI): calcd for $\text{C}_{20}\text{H}_{25}\text{N}_2\text{OS}^+$, 341.1682; found, 341.1681.

2-Ethyl-1-(4-(naphthalen-2-ylthio)butyl)-1H-benzo[d]imidazole.



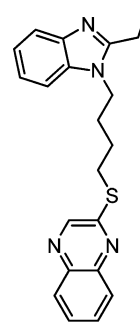
Compound 8: Yield = 66%. ^1H NMR (300 MHz, chloroform-*d*) δ 1.45 (t, J = 7.5 Hz, 3H), 1.63–1.82 (m, 2H), 1.84–2.15 (m, 2H), 2.84 (q, J = 7.5 Hz, 2H), 3.02 (t, J = 6.9 Hz, 2H), 4.08 (t, J = 7.4 Hz, 2H), 7.09–7.32 (m, 3H), 7.32–7.56 (m, 3H), 7.65–7.86 (m, 5H). LCMS-ESI ($M + H$) $^+$: 361.2. HRMS (ESI): calcd for $\text{C}_{23}\text{H}_{25}\text{N}_2\text{S}^+$, 361.1733; found, 361.1738.

2-(4-(2-Ethyl-1H-benzo[d]imidazol-1-yl)butylthio)quinolone.



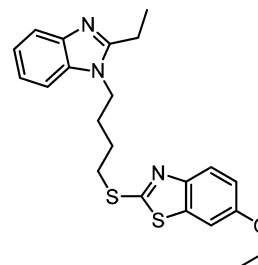
Compound 9: Yield = 66%. ^1H NMR (300 MHz, Chloroform-*d*) δ 1.44 (t, J = 7.5 Hz, 3H), 1.73–2.21 (m, 4H), 2.68–3.04 (m, 2H), 3.24–3.53 (m, 2H), 4.01–4.28 (m, 2H), 7.10–7.51 (m, 5H), 7.55–7.96 (m, 5H). LCMS-ESI ($M+H$) $^+$: 362.2. HRMS (ESI): calcd for $\text{C}_{22}\text{H}_{24}\text{N}_3\text{S}^+$, 362.1685; found, 362.1691.

2-(4-(2-Ethyl-1H-benzo[d]imidazol-1-yl)butylthio)quinoxaline.



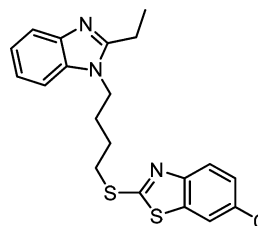
Compound 10: Yield = 78%. ^1H NMR (300 MHz, chloroform-*d*) δ 1.46 (t, J = 7.5 Hz, 3H), 1.77–2.13 (m, 4H), 2.75–3.05 (m, 2H), 3.24–3.49 (m, 2H), 4.03–4.38 (m, 2H), 7.01–7.41 (m, 3H), 7.45–7.94 (m, 4H), 7.89–8.11 (m, 1H), 8.44–8.75 (m, 1H). LCMS-ESI ($M + H$) $^+$: 363.2. HRMS (ESI): calcd for $\text{C}_{21}\text{H}_{23}\text{N}_4\text{S}^+$, 363.1638; found, 363.1643.

6-Ethoxy-2-(4-(2-ethyl-1H-benzo[d]imidazol-1-yl)butylthio)benzo[d]thiazole.



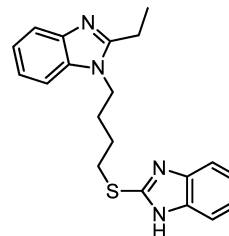
Compound 11: Yield = 60%. ^1H NMR (300 MHz, chloroform-*d*) δ 1.37–1.61 (m, 6H), 1.74–2.31 (m, 4H), 2.63–3.02 (m, 2H), 3.19–3.47 (m, 2H), 3.95–4.29 (m, 4H), 6.84–7.12 (m, 1H), 7.14–7.40 (m, 4H), 7.66–7.88 (m, 2H). LCMS-ESI ($M + H$) $^+$: 412.2. HRMS (ESI): calcd for $\text{C}_{22}\text{H}_{26}\text{N}_3\text{OS}_2^+$, 412.1512; found, 412.1517.

6-Chloro-2-(4-(2-ethyl-1H-benzo[d]imidazol-1-yl)butylthio)benzo[d]thiazole.



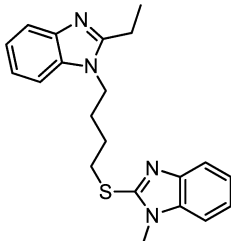
Compound 12: Yield = 84%. ^1H NMR (300 MHz, chloroform-*d*) δ 1.46 (t, J = 7.5 Hz, 3H), 1.80–2.12 (m, 4H), 2.74–3.01 (m, 2H), 3.24–3.48 (m, 2H), 3.96–4.26 (m, 2H), 7.11–7.54 (m, 4H), 7.63–7.96 (m, 3H). LCMS-ESI ($M + H$) $^+$: 402.1. HRMS (ESI): calcd for $\text{C}_{20}\text{H}_{21}\text{ClN}_3\text{S}_2^+$, 402.0860; found, 402.0865.

1-(4-(1H-Benzo[d]imidazol-2-ylthio)butyl)-2-ethyl-1H-benzo[d]imidazole.



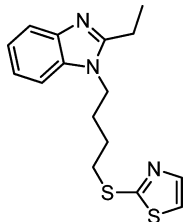
Compound 13: Yield = 77%. ^1H NMR (300 MHz, CDCl_3): δ 1.47 (t, $J = 7.5$ Hz, 3H); 1.93 (m, 4H); 2.85 (q, $J = 7.5$ Hz, 2H); 3.32 (t, $J = 5.4$ Hz, 2H); 4.02 (t, $J = 5.7$ Hz, 2H); 7.15–8.02 (m, 8H). LCMS-ESI ($\text{M} + \text{H}$) $^+$: 351.2. HRMS (ESI): calcd for $\text{C}_{20}\text{H}_{23}\text{N}_4\text{S}^+$, 351.1638; found, 351.1643.

2-Ethyl-1-(4-((1-methyl-1H-benzo[d]imidazol-2-yl)thio)butyl)-1H-benzo[d]imidazole.



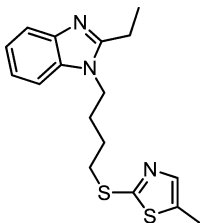
Compound 14: Yield = 99%. ^1H NMR (300 MHz, chloroform- d) δ 1.45 (t, $J = 7.5$ Hz, 3H), 1.78–2.06 (m, 4H), 2.79–2.91 (m, 2H), 3.29–3.49 (m, 2H), 3.65 (s, 3H), 3.98–4.24 (m, 2H), 7.09–7.38 (m, 6H), 7.54–7.82 (m, 2H). LCMS-ESI ($\text{M} + \text{H}$) $^+$: 365.2. HRMS (ESI): calcd for $\text{C}_{21}\text{H}_{23}\text{N}_4\text{S}^+$, 365.1794; found, 365.1800.

2-(4-(2-Ethyl-1H-benzo[d]imidazol-1-yl)butylthio)thiazole.



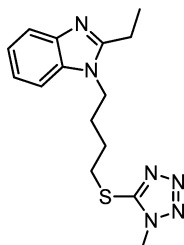
Compound 15: Yield = 79%. ^1H NMR (300 MHz, chloroform- d) δ 1.47 (t, $J = 7.4$ Hz, 3H), 1.75–2.11 (m, 4H), 2.59–3.06 (m, 2H), 3.12–3.38 (m, 2H), 3.97–4.23 (m, 2H), 7.13–7.35 (m, 4H), 7.58–7.79 (m, 2H). LCMS-ESI ($\text{M} + \text{H}$) $^+$: 318.1. HRMS (ESI): calcd for $\text{C}_{16}\text{H}_{20}\text{N}_3\text{S}_2^+$, 318.1093; found, 318.1099.

2-(4-(2-Ethyl-1H-benzo[d]imidazol-1-yl)butylthio)-5-methylthiazole.



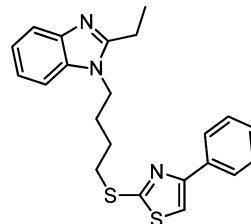
Compound 16: Yield 50%. ^1H NMR (300 MHz, chloroform- d) δ 1.47 (t, $J = 7.5$ Hz, 3H), 1.74–2.04 (m, 4H), 2.72 (s, 3H), 2.88 (q, $J = 7.5$ Hz, 2H), 3.32 (t, $J = 6.8$ Hz, 2H), 4.13 (t, $J = 7.0$ Hz, 2H), 7.18–7.38 (m, 4H), 7.65–7.77 (m, 1H). LCMS-ESI ($\text{M} + \text{H}$) $^+$: 332.9. HRMS (ESI): calcd for $\text{C}_{17}\text{H}_{22}\text{N}_3\text{S}_2^+$, 332.1250; found, 332.1255.

2-Ethyl-1-(4-((1-methyl-1H-tetrazol-5-yl)thio)butyl)-1H-benzo[d]imidazole.



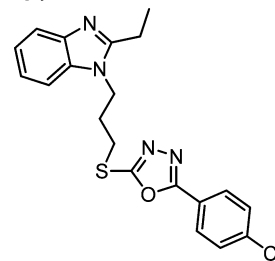
Compound 17: Yield = 95%. ^1H NMR (300 MHz, chloroform- d) δ 1.47 (t, $J = 7.5$ Hz, 3H), 1.78–2.06 (m, 4H), 2.77–3.01 (m, 2H), 3.33 (t, $J = 6.7$ Hz, 2H), 3.86 (s, 3H), 4.13 (t, $J = 6$ Hz, 2H), 7.25 (m, 3H), 7.64–7.83 (m, 1H). LCMS-ESI ($\text{M} + \text{H}$) $^+$: 317.2. HRMS (ESI): calcd for $\text{C}_{15}\text{H}_{21}\text{N}_6\text{S}^+$, 317.1543; found, 317.1548.

2-((4-(2-Ethyl-1H-benzo[d]imidazol-1-yl)butyl)thio)-4-phenylthiazole.



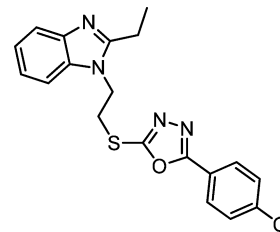
Compound 18: Yield = 90%. ^1H NMR (300 MHz, CDCl_3): 1.46 (t, $J = 7.5$ Hz, 3H); 1.94 (m, 4H); 2.88 (q, $J = 7.2$ Hz, 2H); 3.28 (t, $J = 7$ Hz, 2H); 4.10 (t, $J = 7$ Hz, 2H); 7.19–7.64 (m, 10H). LCMS-ESI ($\text{M} + \text{H}$) $^+$: 394.2. HRMS (ESI): calcd for $\text{C}_{22}\text{H}_{24}\text{N}_3\text{S}_2^+$, 394.1406; found, 394.1412.

2-(4-Chlorophenyl)-5-((3-(2-ethyl-1H-benzo[d]imidazol-1-yl)propyl)thio)-1,3,4-oxadiazole.



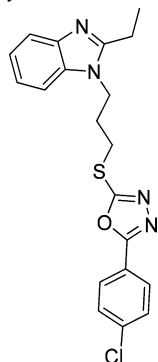
Compound 20: Yield = 50%. ^1H NMR (300 MHz, CDCl_3): δ 1.49 (t, $J = 7.5$ Hz, 3H); 2.41 (m, 2H); 2.94 (q, $J = 6.8$ Hz, 2H); 3.30 (t, $J = 6.9$ Hz, 2H); 4.31 (t, $J = 7.2$ Hz, 2H); 7.22–7.94 (m, 8H). LCMS-ESI ($\text{M} + \text{H}$) $^+$: 399.2. HRMS (ESI): calcd for $\text{C}_{20}\text{H}_{20}\text{ClN}_4\text{OS}^+$, 399.1041; found, 399.1047.

2-(4-Chlorophenyl)-5-((2-(2-ethyl-1H-benzo[d]imidazol-1-yl)ethyl)thio)-1,3,4-oxadiazole.



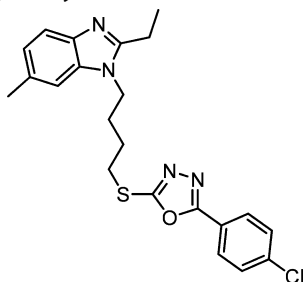
Compound 21: Yield = 71%. ^1H NMR (300 MHz, chloroform- d) δ 1.50 (t, $J = 7.5$ Hz, 3H), 2.97 (q, $J = 7.5$ Hz, 2H), 3.60 (t, $J = 6.9$ Hz, 2H), 4.66 (t, $J = 7.2$ Hz, 2H), 7.18–7.33 (m, 2H), 7.44–7.55 (m, 4H), 7.68–7.80 (m, 1H), 7.94 (d, $J = 8.6$ Hz, 2H). LCMS-ESI ($\text{M} + \text{H}$) $^+$: 385.10. HRMS (ESI): calcd for $\text{C}_{19}\text{H}_{18}\text{ClN}_4\text{OS}^+$, 385.0884; found, 385.0894.

2-(4-Chlorophenyl)-5-((3-(2-ethyl-6-methyl-1H-benzo[d]imidazol-1-yl)propyl)thio)-1,3,4-oxadiazole.



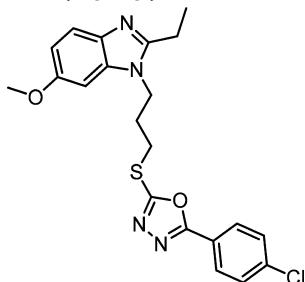
Compound 22: Yield = 38%. $^1\text{H NMR}$ (300 MHz, CDCl_3): δ 1.45 (t, $J = 7.5$ Hz, 3H); 2.47 (m, 2H); 2.88 (q, $J = 7.0$ Hz, 2H); 3.29 (t, $J = 6.6$ Hz, 2H); 4.28 (t, $J = 7.5$ Hz, 2H); 7.04–7.94 (m, 7H). LCMS-ESI ($\text{M} + \text{H}$) $^+$: 413.1. HRMS (ESI): calcd for $\text{C}_{21}\text{H}_{22}\text{ClN}_4\text{OS}^+$, 413.1197; found, 413.1203.

2-(4-Chlorophenyl)-5-((4-(2-ethyl-6-methyl-1H-benzo[d]imidazol-1-yl)butyl)thio)-1,3,4-oxadiazole.



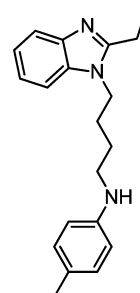
Compound 23: Yield = 31%. $^1\text{H NMR}$ (300 MHz, CDCl_3): δ 1.45 (t, $J = 7.5$ Hz, 3H); 1.98 (m, 4H); 2.47 (s, 3H); 2.88 (q, $J = 6.7$ Hz, 2H); 3.30 (t, $J = 7.0$ Hz, 2H); 4.13 (t, $J = 7.5$ Hz, 2H); 7.03–7.95 (m, 7H). LCMS-ESI ($\text{M} + \text{H}$) $^+$: 427.1. HRMS (ESI): calcd for $\text{C}_{22}\text{H}_{24}\text{ClN}_4\text{OS}^+$, 427.1354; found, 427.1359.

2-(4-Chlorophenyl)-5-((3-(2-ethyl-6-methoxy-1H-benzo[d]imidazol-1-yl)propyl)thio)-1,3,4-oxadiazole.



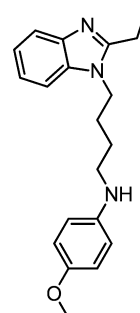
Compound 24: Yield = 63%. $^1\text{H NMR}$ (300 MHz, chloroform-*d*): δ 1.48 (t, $J = 7.5$ Hz, 3H), 2.32–2.54 (m, 2H), 2.83–2.94 (m, 2H), 3.30 (t, $J = 7.0$ Hz, 2H), 3.87 (s, 3H), 4.26 (t, $J = 7.1$ Hz, 2H), 6.73–6.93 (m, 2H), 7.49 (d, $J = 8.6$ Hz, 2H), 7.62 (d, $J = 8.7$ Hz, 1H), 7.93 (d, $J = 8.6$ Hz, 2H). LCMS-ESI ($\text{M} + \text{H}$) $^+$: 428.9. HRMS (ESI): calcd for $\text{C}_{21}\text{H}_{22}\text{ClN}_4\text{O}_2\text{S}^+$, 429.1147; found, 429.1155.

***N*-(4-(2-Ethyl-1H-benzo[d]imidazol-1-yl)butyl)-4-methylaniline.**



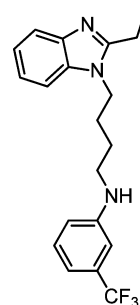
Compound 25: Yield = 27%. $^1\text{H NMR}$ (300 MHz, chloroform-*d*) δ 1.47 (t, $J = 7.3$ Hz, 3H), 1.60–1.80 (m, 2H), 1.81–1.99 (m, 2H), 2.24 (s, 3H), 2.89 (q, $J = 7.3$ Hz, 2H), 3.13 (t, $J = 6.6$ Hz, 2H), 3.44 (broad s, 1H), 4.14 (t, $J = 7.1$ Hz, 2H), 6.51 (d, $J = 8.0$ Hz, 2H), 6.99 (d, $J = 7.7$ Hz, 2H), 7.14–7.37 (m, 3H), 7.64–7.87 (m, 1H). LCMS-ESI ($\text{M} + \text{H}$) $^+$: 308.2. HRMS (ESI): calcd for $\text{C}_{20}\text{H}_{26}\text{N}_3^+$, 308.2121; found, 308.2119.

***N*-(4-(2-Ethyl-1H-benzo[d]imidazol-1-yl)butyl)-4-methoxyaniline.**

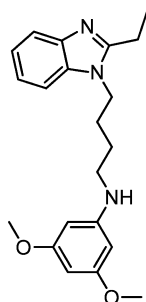


Compound 26: Yield = 82%. $^1\text{H NMR}$ (300 MHz, chloroform-*d*) δ 1.49 (t, $J = 7.5$ Hz, 3H), 1.57–1.76 (m, 2H), 1.84–2.07 (m, 2H), 2.90 (q, $J = 7.5$ Hz, 2H), 3.11 (t, $J = 6.9$ Hz, 2H), 3.76 (s, 4H), 4.15 (t, $J = 7.3$ Hz, 2H), 6.57 (d, $J = 8.8$ Hz, 2H), 6.80 (d, $J = 8.8$ Hz, 2H), 7.09–7.35 (m, 3H), 7.63–7.82 (m, 1H). LCMS-ESI ($\text{M} + \text{H}$) $^+$: 324.0. HRMS (ESI): calcd for $\text{C}_{20}\text{H}_{26}\text{N}_3\text{O}^+$, 324.2070; found, 324.2081.

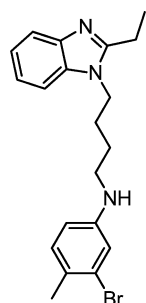
***N*-(4-(2-Ethyl-1H-benzo[d]imidazol-1-yl)butyl)-3-(trifluoromethyl)aniline.**



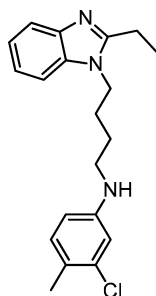
Compound 27: Yield = 53%. $^1\text{H NMR}$ (300 MHz, chloroform-*d*) δ 1.50 (t, $J = 7.4$ Hz, 3H), 1.57–1.80 (m, 2H), 1.80–2.10 (m, 2H), 2.91 (q, $J = 7.2$ Hz, 2H), 3.00–3.28 (m, 2H), 3.80 (broad s, 1H), 4.00–4.28 (m, 2H), 6.50–6.84 (m, 2H), 6.80–7.05 (m, 1H), 7.04–7.43 (m, 4H), 7.60–7.85 (m, 1H). LCMS-ESI ($\text{M} + \text{H}$) $^+$: 362.2. HRMS (ESI): calcd for $\text{C}_{20}\text{H}_{23}\text{F}_3\text{N}_3^+$, 362.1839; found, 362.1834.

***N*-(4-(2-Ethyl-1H-benzo[d]imidazol-1-yl)butyl)-3,5-dimethoxyaniline.**

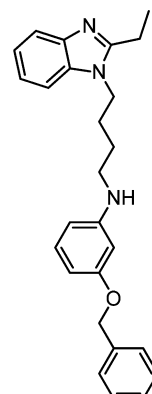
Compound 28: Yield = 73%. $^1\text{H NMR}$ (300 MHz, chloroform-*d*) δ 1.49 (t, J = 7.4 Hz, 3H), 1.57–1.76 (m, 2H), 1.79–1.99 (m, 2H), 2.80–2.95 (m, 2H), 3.13 (t, J = 7.1 Hz, 2H), 3.76 (broad s, 6 H), 4.14 (t, J = 7.1 Hz, 2H), 5.68–5.99 (m, 3H), 7.07–7.35 (m, 3H), 7.66–7.87 (m, 1H). LCMS-ESI ($M + H$) $^+$: 354.2. HRMS (ESI): calcd for $\text{C}_{21}\text{H}_{28}\text{N}_3\text{O}_2$ $^+$, 354.2176; found, 354.2156.

3-Bromo-*N*-(4-(2-Ethyl-1H-benzo[d]imidazol-1-yl)butyl)-4-methylaniline.

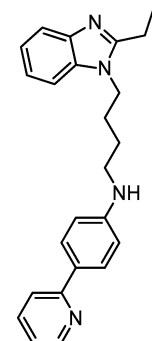
Compound 29: Yield = 56%. $^1\text{H NMR}$ (300 MHz, chloroform-*d*) δ 1.49 (t, J = 7.5 Hz, 3H), 1.79–2.09 (m, 4H), 2.90 (q, J = 7.9 Hz, 2H), 3.41 (t, J = 6.8 Hz, 2H), 3.74 (broad s, 1H), 4.14 (t, J = 6.7 Hz, 2H), 7.03–7.38 (m, 5H), 7.38–7.89 (m, 2H). LCMS-ESI ($M + H$) $^+$: 386.1. HRMS (ESI): calcd for $\text{C}_{20}\text{H}_{25}\text{BrN}_3$ $^+$, 386.1226; found, 386.1224.

3-Chloro-*N*-(4-(2-ethyl-1H-benzo[d]imidazol-1-yl)butyl)-4-methylaniline.

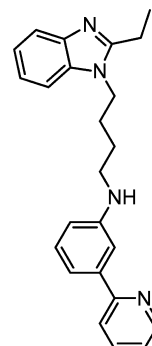
Compound 30: Yield = 51%. $^1\text{H NMR}$ (300 MHz, chloroform-*d*) δ 1.50 (t, J = 7.5 Hz, 3H), 1.59–1.78 (m, 2H), 1.78–2.00 (m, 2H), 2.26 (s, 3H), 2.90 (q, J = 7.5 Hz, 2H), 3.12 (t, J = 6.9 Hz, 2H), 3.53 (broad s, 1H), 4.15 (t, J = 7.3 Hz, 2H), 6.40 (d, J = 8.4 Hz, 1H), 6.60 (d, J = 2.5 Hz, 1H), 7.00 (d, J = 8.2 Hz, 1H), 7.17–7.36 (m, 3H), 7.58–7.84 (m, 1H). LCMS-ESI ($M + H$) $^+$: 342.0. HRMS (ESI): calcd for $\text{C}_{20}\text{H}_{25}\text{ClN}_3$ $^+$, 342.1732; found, 342.1733.

3-(Benzyloxy)-*N*-(4-(2-ethyl-1H-benzo[d]imidazol-1-yl)butyl)aniline.

Compound 31: Yield = 48%. $^1\text{H NMR}$ (300 MHz, chloroform-*d*) δ 1.46 (t, J = 7.5 Hz, 3H), 1.53–1.71 (m, 2H), 1.73–1.96 (m, 2H), 2.86 (q, J = 7.5 Hz, 2H), 3.10 (t, J = 6.9 Hz, 2H), 3.61 (broad s, 1H), 4.10 (t, J = 7.3 Hz, 2H), 5.01 (s, 2H), 6.08–6.26 (m, 2H), 6.28–6.40 (m, 1H), 6.93–7.12 (m, 1H), 7.18–7.49 (m, 7H), 7.65–7.80 (m, 1H). LCMS-ESI ($M + H$) $^+$: 400.2. HRMS (ESI): calcd for $\text{C}_{26}\text{H}_{30}\text{N}_3\text{O}^+$, 400.2383; found, 400.2389.

***N*-(4-(2-Ethyl-1H-benzo[d]imidazol-1-yl)butyl)-4-(pyridin-2-yl)aniline.**

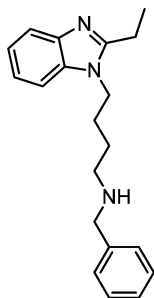
Compound 32: Yield = 42%. $^1\text{H NMR}$ (300 MHz, chloroform-*d*) δ 1.47 (t, J = 7.5 Hz, 3H), 1.59–1.80 (m, 2H), 1.82–2.06 (m, 2H), 2.88 (q, J = 7.5 Hz, 2H), 3.09–3.30 (m, 3H), 4.07–4.24 (m, 2H), 6.58–6.71 (m, 2H), 7.03–7.16 (m, 1H), 7.17–7.34 (m, 3H), 7.57–7.78 (m, 3H), 7.79–7.90 (m, 2H), 8.53–8.66 (m, 1H). LCMS-ESI ($M + H$) $^+$: 371.2. HRMS (ESI): calcd for $\text{C}_{24}\text{H}_{27}\text{N}_4$ $^+$, 371.2230; found, 371.2229.

***N*-(4-(2-Ethyl-1H-benzo[d]imidazol-1-yl)butyl)-3-(pyridin-2-yl)aniline.**

Compound 33: Yield = 50%. $^1\text{H NMR}$ (300 MHz, chloroform-*d*) δ 1.49 (t, J = 7.5 Hz, 3H), 1.59–1.82 (m, 2H), 1.79–2.10 (m, 2H), 2.91 (q, J = 8.1 Hz, 2H), 3.10–3.38 (m, 2H), 3.74 (broad s,

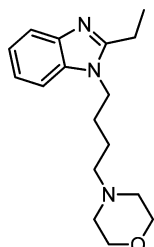
1H), 3.99–4.28 (m, 2H), 6.48–6.75 (m, 1H), 7.04–7.42 (m, 7H), 7.48–7.84 (m, 3H), 8.53–8.82 (m, 1H). LCMS-ESI (M + H)⁺: 371.2. HRMS (ESI): calcd for C₂₄H₂₇N₄⁺, 371.2230; found, 371.2219.

N-Benzyl-4-(2-ethyl-1H-benzo[d]imidazol-1-yl)butan-1-amine.



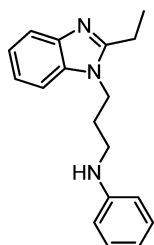
Compound 34: Yield = 81%. ¹H NMR (300 MHz, chloroform-*d*) δ 1.46 (t, *J* = 7.5 Hz, 3H), 1.59–2.03 (m, 4H), 2.88 (q, *J* = 7.5 Hz, 2H), 3.50 (t, *J* = 6.9 Hz, 2H), 4.13 (t, *J* = 7.0 Hz, 2H), 4.49 (s, 2H), 7.09–7.43 (m, 8H), 7.54–7.84 (m, 1H). LCMS-ESI (M + H)⁺: 308.2. HRMS (ESI): calcd for C₂₀H₂₆N₃⁺, 308.2121; found, 308.2127.

4-(4-(2-Ethyl-1H-benzo[d]imidazol-1-yl)butyl)-morpholine.



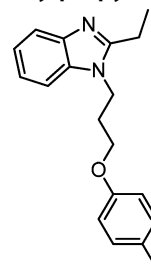
Compound 35: Yield = 64%. ¹H NMR (300 MHz, chloroform-*d*) δ 1.42 (t, *J* = 7.5 Hz, 3H), 1.46–1.66 (m, 2H), 1.72–1.94 (m, 2H), 2.23–2.56 (m, 6H), 2.95 (q, *J* = 7.5 Hz, 2H), 3.53–3.72 (m, 4H), 4.24 (t, *J* = 7.4 Hz, 2H), 7.17–7.33 (m, 2H), 7.47 (d, *J* = 7.6 Hz, 1H), 7.58 (d, *J* = 8.4 Hz, 1H). LCMS-ESI (M + H)⁺: 288.2. HRMS (ESI): calcd for C₁₇H₂₆N₃O⁺, 288.2070; found, 288.2073.

N-(3-(2-Ethyl-1H-benzo[d]imidazol-1-yl)propyl)-aniline.



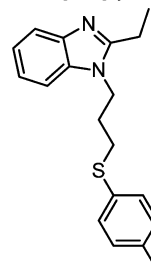
Compound 37: Yield = 29%. ¹H NMR (300 MHz, chloroform-*d*) δ 1.45 (t, *J* = 7.5 Hz, 3H), 2.13 (m, 2H), 2.88 (q, *J* = 7.5 Hz, 2H), 3.18 (t, *J* = 6.5 Hz, 2H), 3.59 (broad s, 1H), 4.26 (t, *J* = 7.0 Hz, 2H), 6.58 (d, *J* = 8.5 Hz, 2H), 6.74 (t, *J* = 7.3 Hz, 1H), 6.99–7.37 (m, 5H), 7.63–7.86 (m, 1H). LCMS-ESI (M + H)⁺: 280.2. HRMS (ESI): calcd for C₁₈H₂₂N₃⁺, 280.1808; found, 280.1814.

2-Ethyl-1-(3-(p-tolyloxy)propyl)-1H-benzo[d]imidazole.



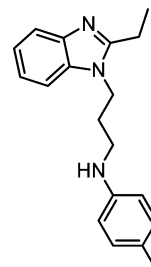
Compound 38: Yield = 80%. ¹H NMR (300 MHz, chloroform-*d*) δ 1.43 (t, *J* = 7.5 Hz, 3H), 2.18–2.37 (m, 2H), 2.88 (q, *J* = 7.4 Hz, 2H), 3.88 (t, *J* = 6.5 Hz, 2H), 4.35 (t, *J* = 6.6 Hz, 2H), 6.78 (d, *J* = 8.3 Hz, 2H), 7.08 (d, *J* = 8.0 Hz, 2H), 7.13–7.39 (m, 3H), 7.73 (m, 1H). LCMS-ESI (M + H)⁺: 295.2. HRMS (ESI): calcd for C₁₉H₂₃ON₂⁺, 295.1805; found, 295.1803.

2-Ethyl-1-(3-(p-tolythio)propyl)-1H-benzo[d]imidazole.



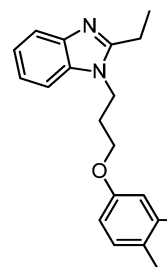
Compound 39: Yield = 54%. ¹H NMR (300 MHz, chloroform-*d*) δ 1.44 (t, *J* = 7.5 Hz, 3H), 1.87–2.21 (m, 2H), 2.32 (s, 3H), 2.74–2.99 (m, 4H), 4.09–4.38 (m, 2H), 7.01–7.38 (m, 7H), 7.61–7.82 (m, 1H). LCMS-ESI (M + H)⁺: 311.1. HRMS (ESI): calcd for C₁₉H₂₃N₂S⁺, 311.1576; found, 311.1574.

N-(3-(2-Ethyl-1H-benzo[d]imidazol-1-yl)propyl)-4-methylaniline.



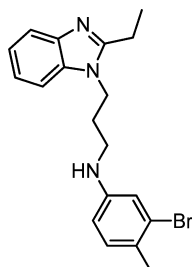
Compound 40: Yield = 48%. ¹H NMR (300 MHz, chloroform-*d*) δ 1.45 (t, *J* = 7.4 Hz, 3H), 2.11 (m, 2H), 2.24 (s, 3H), 2.87 (q, *J* = 7.4 Hz, 2H), 3.14 (t, *J* = 6.8 Hz, 2H), 3.47 (broad s, 1H), 4.24 (t, *J* = 6.9 Hz, 2H), 6.51 (d, *J* = 8.7 Hz, 2H), 6.99 (d, *J* = 7.7 Hz, 2H), 7.11–7.38 (m, 3H), 7.60–7.84 (m, 1H). LCMS-ESI (M + H)⁺: 294.2. HRMS (ESI): calcd for C₁₉H₂₄N₃⁺, 294.1965; found, 294.1969.

1-(3-(3,4-Dimethylphenoxy)propyl)-2-ethyl-1H-benzo[d]imidazole.



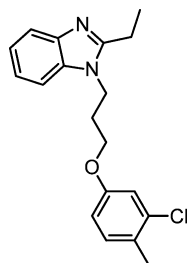
Compound 41: Yield = 74%. $^1\text{H NMR}$ (300 MHz, chloroform-*d*) δ 1.43 (t, $J = 7.5$ Hz, 3H), 2.03–2.38 (m, 8H), 2.88 (q, $J = 7.4$ Hz, 2H), 3.88 (t, $J = 6.2$ Hz, 2H), 4.34 (t, $J = 6.7$ Hz, 2H), 6.54–6.66 (m, 1H), 6.69 (s, 1H), 7.03 (d, $J = 8.2$ Hz, 1H), 7.12–7.27 (m, 2H), 7.30–7.41 (m, 1H), 7.73 (d, $J = 7.1$ Hz, 1H). LCMS-ESI ($M + H$) $^+$: 309.3. HRMS (ESI): calcd for $\text{C}_{20}\text{H}_{25}\text{N}_2\text{O}^+$, 309.1961; found, 309.1957.

3-Bromo-*N*-(3-(2-ethyl-1H-benzo[d]imidazol-1-yl)propyl)-4-methylaniline.



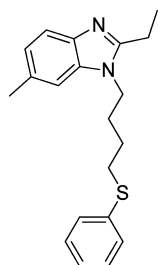
Compound 42: Yield = 26%. $^1\text{H NMR}$ (300 MHz, chloroform-*d*) δ 1.46 (t, $J = 7.5$ Hz, 3H), 1.97–2.21 (m, 2H), 2.28 (s, 3H), 2.87 (q, $J = 7.2$ Hz, 2H), 3.12 (t, $J = 6.4$ Hz, 2H), 4.24 (t, $J = 6.5$ Hz, 2H), 6.42 (d, $J = 8.2$ Hz, 1H), 6.79 (s, 1H), 7.00 (d, $J = 8.1$ Hz, 1H), 7.15–7.44 (m, 3H), 7.75 (d, $J = 7.2$ Hz, 1H). LCMS-ESI ($M + H$) $^+$: 371.9. HRMS (ESI): calcd for $\text{C}_{19}\text{H}_{23}\text{BrN}_3^+$, 372.1070; found, 372.1055.

1-(3-(3-Chloro-4-methylphenoxy)propyl)-2-ethyl-1H-benzo[d]imidazole.



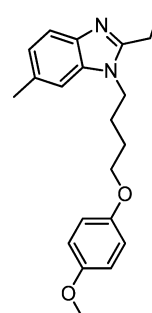
Compound 43: Yield = 80%. $^1\text{H NMR}$ (300 MHz, chloroform-*d*) δ 1.43 (t, $J = 7.5$ Hz, 3H), 2.18–2.28 (m, 2H), 2.30 (s, 3H), 2.87 (q, $J = 7.5$ Hz, 2H), 3.86 (t, $J = 6.5$ Hz, 2H), 4.33 (t, $J = 6.8$ Hz, 2H), 6.69 (d, $J = 8.4$ Hz, 1H), 6.89 (d, $J = 2.3$ Hz, 1H), 7.11 (d, $J = 8.5$ Hz, 1H), 7.18–7.36 (m, 3H), 7.74 (d, $J = 8.2$ Hz, 1H). LCMS-ESI ($M + H$) $^+$: 329.2. HRMS (ESI): calcd for $\text{C}_{19}\text{H}_{22}\text{ClN}_2\text{O}^+$, 329.1415; found, 329.1406.

2-Ethyl-6-methyl-1-(4-(phenylthio)butyl)-1H-benzo[d]imidazole.



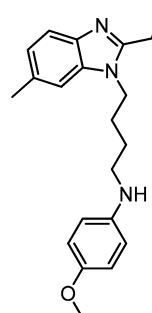
Compound 45: Yield = 21%. $^1\text{H NMR}$ (300 MHz, chloroform-*d*) δ 1.45 (t, $J = 7.5$ Hz, 3H), 1.56–1.83 (m, 2H), 1.84–2.13 (m, 2H), 2.48 (s, 3H), 2.74–3.06 (m, 4H), 3.92–4.23 (m, 2H), 6.96–7.40 (m, 6H), 7.45–7.72 (m, 1H). LCMS-ESI ($M + H$) $^+$: 325.2.

2-Ethyl-1-(4-(4-methoxyphenoxy)butyl)-6-methyl-1H-benzo[d]imidazole.



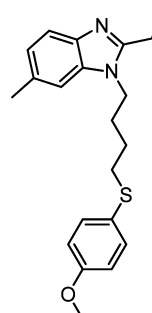
Compound 47: Yield = 70%. $^1\text{H NMR}$ (300 MHz, chloroform-*d*) δ 1.48 (t, $J = 7.5$ Hz, 3H), 1.72–1.93 (m, 2H), 1.92–2.11 (m, 2H), 2.49 (s, 3H), 2.90 (q, $J = 7.5$ Hz, 2H), 3.78 (s, 3H), 3.86–4.00 (m, 2H), 4.10–4.27 (m, 2H), 6.73–6.96 (m, 4H), 6.99–7.25 (m, 2H), 7.47–7.69 (m, 1H). LCMS-ESI ($M + H$) $^+$: 339.0. HRMS (ESI): calcd for $\text{C}_{21}\text{H}_{27}\text{N}_2\text{O}_2^+$, 339.2067; found, 339.2064.

***N*-(4-(2-Ethyl-6-methyl-1H-benzo[d]imidazol-1-yl)butyl)-4-methoxyaniline.**

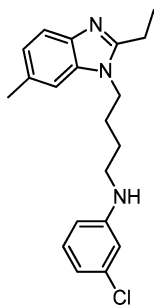


Compound 48: Yield = 70%. $^1\text{H NMR}$ (300 MHz, chloroform-*d*) δ 1.46 (t, $J = 7.4$ Hz, 3H), 1.59–1.80 (m, 2H), 1.81–2.01 (m, 2H), 2.49 (s, 3H), 2.78–2.94 (m, 3H), 3.11 (q, $J = 6.5$ Hz, 2H), 3.76 (s, 3H), 3.99–4.26 (m, 2H), 6.37–6.68 (m, 2H), 6.79 (d, $J = 7.8$ Hz, 2H), 7.06 (d, $J = 8.0$ Hz, 2H), 7.48–7.75 (m, 1H). LCMS-ESI ($M + H$) $^+$: 338.1. HRMS (ESI): calcd for $\text{C}_{21}\text{H}_{28}\text{N}_3\text{O}^+$, 338.2227; found, 338.2221.

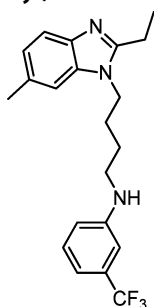
2-Ethyl-1-(4-((4-methoxyphenyl)thio)butyl)-6-methyl-1H-benzo[d]imidazole.



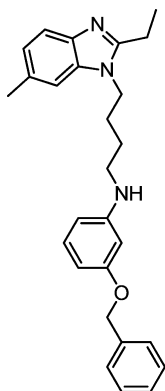
Compound 49: Yield = 80%. $^1\text{H NMR}$ (300 MHz, chloroform-*d*) δ 1.46 (t, $J = 7.5$ Hz, 3H), 1.52–1.73 (m, 2H), 1.83–2.02 (m, 2H), 2.50 (s, 3H), 2.75–2.93 (m, 4H), 3.80 (s, 3H), 3.94–4.17 (m, 2H), 6.58–6.90 (m, 2H), 6.98–7.22 (m, 2H), 7.22–7.38 (m, 2H), 7.46–7.69 (m, 1H). LCMS-ESI ($M + H$) $^+$: 355.0. HRMS (ESI): calcd for $\text{C}_{21}\text{H}_{27}\text{N}_2\text{OS}^+$, 355.1839; found, 355.1835.

3-Chloro-*N*-(4-(2-ethyl-6-methyl-1H-benzo[d]imidazol-1-yl)butyl)aniline.

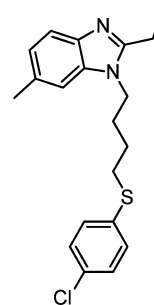
Compound **50**: Yield = 15%. $^1\text{H NMR}$ (300 MHz, CDCl_3): δ 1.45 (t, $J = 7.5$ Hz, 3H); 1.62 (m, 2H); 1.90 (m, 2H); 2.49 (s, 3H); 2.86 (q, $J = 7.5$ Hz, 2H); 3.40 (broad s, 1H); 3.54 (t, $J = 6.9$ Hz, 2H); 4.13 (t, $J = 6.7$ Hz, 2H); 7.06–7.62 (m, 7H). LCMS-ESI ($\text{M} + \text{H}$) $^+$: 342.0.

***N*-(4-(2-Ethyl-6-methyl-1H-benzo[d]imidazol-1-yl)-propyl)-3-(trifluoromethyl)aniline.**

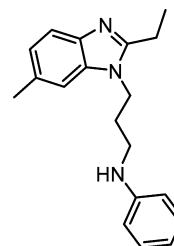
Compound **51**: Yield = 27%. $^1\text{H NMR}$ (300 MHz, CDCl_3): δ 1.45 (t, $J = 7.5$ Hz, 3H); 1.66 (m, 2H); 1.90 (m, 2H); 2.47 (s, 3H); 2.86 (q, $J = 7.5$ Hz, 2H); 3.08 (t, $J = 6.9$ Hz, 2H); 3.70 (broad s, 1H); 4.13 (t, $J = 5.7$ Hz, 2H); 6.68–8.01 (m, 7H). LCMS-ESI ($\text{M} + \text{H}$) $^+$: 376.2. HRMS (ESI): calcd for $\text{C}_{21}\text{H}_{25}\text{F}_3\text{N}_3^+$, 376.1995; found, 376.1979.

3-(Benzoyloxy)-*N*-(4-(2-ethyl-6-methyl-1H-benzo[d]imidazol-1-yl)butyl)aniline.

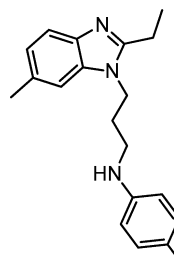
Compound **52**: Yield = 43%. $^1\text{H NMR}$ (300 MHz, chloroform-*d*) δ 1.45 (t, $J = 7.2$ Hz, 3H), 1.53–1.99 (m, 4H), 2.48 (s, 3H), 2.74–2.92 (m, 2H), 3.12 (q, $J = 6.4$ Hz, 2H), 3.61 (broad s, 1H), 3.99–4.19 (m, 2H), 5.02 (s, 2H), 5.99–6.30 (m, 2H), 6.35 (d, $J = 8.6$ Hz, 1H), 6.95–7.68 (m, 9H). LCMS-ESI ($\text{M} + \text{H}$) $^+$: 414.3. HRMS (ESI): calcd for $\text{C}_{27}\text{H}_{32}\text{N}_3\text{O}^+$, 414.2540; found, 414.2531.

1-(4-(4-Chlorophenylthio)butyl)-2-ethyl-6-methyl-1H-benzo[d]imidazole.

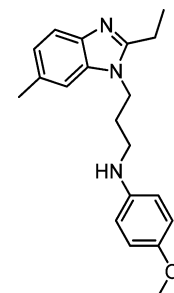
Compound **53**: Yield = 89%. $^1\text{H NMR}$ (300 MHz, chloroform-*d*) δ 1.44 (t, $J = 7.5$ Hz, 3H), 1.57–1.77 (m, 2H), 1.84–2.04 (m, 2H), 2.48 (s, 3H), 2.66–2.98 (m, 4H), 4.05 (t, $J = 8.8$ Hz, 2H), 6.99–7.31 (m, 6H), 7.46–7.68 (m, 1H). LCMS-ESI ($\text{M} + \text{H}$) $^+$: 359.1. HRMS (ESI): calcd for $\text{C}_{20}\text{H}_{24}\text{ClN}_2\text{S}^+$, 359.1343; found, 359.1349.

***N*-(3-(2-Ethyl-6-methyl-1H-benzo[d]imidazol-1-yl)-propyl)aniline.**

Compound **54**: Yield = 61%. $^1\text{H NMR}$ (300 MHz, chloroform-*d*) δ 1.46 (t, $J = 7.5$ Hz, 3H), 1.98–2.26 (m, 2H), 2.45 (s, 3H), 2.87 (q, $J = 7.5$ Hz, 2H), 3.19 (t, $J = 6.1$ Hz, 2H), 3.64 (s, 1H), 4.23 (t, $J = 7.0$ Hz, 2H), 6.60 (d, $J = 7.7$ Hz, 2H), 6.76 (t, $J = 7.3$ Hz, 1H), 6.98–7.13 (m, 2H), 7.21 (t, $J = 7.9$ Hz, 2H), 7.63 (d, $J = 8.6$ Hz, 1H). LCMS-ESI ($\text{M} + \text{H}$) $^+$, 294.1

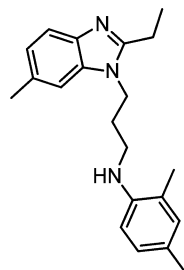
***N*-(3-(2-Ethyl-6-methyl-1H-benzo[d]imidazol-1-yl)-propyl)-4-methylaniline.**

Compound **55**: Yield = 23%. $^1\text{H NMR}$ (300 MHz, chloroform-*d*) δ 1.44 (t, $J = 7.5$ Hz, 3H), 1.90–2.20 (m, 2H), 2.28 (s, 3H), 2.47 (s, 3H), 2.85 (q, $J = 7.5$ Hz, 2H), 3.01–3.22 (m, 2H), 4.06–4.30 (m, 2H), 6.28–6.51 (m, 1H), 6.67–6.79 (m, 1H), 6.96–7.25 (m, 3H), 7.45–7.70 (m, 2H). LCMS-ESI ($\text{M} + \text{H}$) $^+$: 308.2.

***N*-(3-(2-Ethyl-6-methyl-1H-benzo[d]imidazol-1-yl)-propyl)-4-methoxyaniline.**

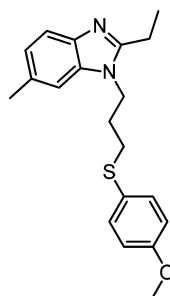
Compound **56**: Yield = 42%. $^1\text{H NMR}$ (300 MHz, CDCl_3): δ 1.44 (t, $J = 7.5$ Hz, 3H); 2.04 (m, 2H); 2.47 (s, 3H); 2.91 (m, 4H); 3.81 (s, 3H); 4.22 (t, $J = 7.2$ Hz, 2H); 6.84–7.61 (m, 7H). LCMS-ESI ($M + H$) $^+$: 324.1. HRMS (ESI): calcd for $\text{C}_{20}\text{H}_{26}\text{N}_3\text{O}^+$, 324.2070; found, 324.2084.

***N*-(3-(2-Ethyl-6-methyl-1H-benzo[d]imidazol-1-yl)propyl)-2,4-dimethylaniline.**



Compound **57**: Yield = 28%. $^1\text{H NMR}$ (300 MHz, CDCl_3): δ 1.45 (t, $J = 2.4$ Hz, 3H); 2.19 (m, 8H); 2.47 (s, 3H); 2.88 (q, $J = 6.7$ Hz, 2H); 3.17 (t, $J = 6.6$ Hz, 2H); 3.50 (s, 1H); 4.23 (t, $J = 7.2$ Hz, 2H); 6.41–7.61 (m, 6H). LCMS-ESI ($M + H$) $^+$: 322.2. HRMS (ESI): calcd for $\text{C}_{21}\text{H}_{28}\text{N}_3^+$, 322.2283; found, 322.2276.

2-Ethyl-1-(3-((4-methoxyphenyl)thio)propyl)-6-methyl-1H-benzo[d]imidazole.



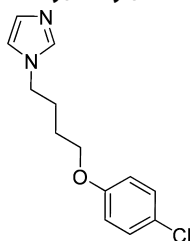
Compound **58**: Yield = 62%. $^1\text{H NMR}$ (300 MHz, chloroform-*d*) δ 1.44 (t, $J = 7.5$ Hz, 3H), 1.94–2.15 (m, 2H), 2.47 (s, 3H), 2.71–2.97 (m, 4H), 3.81 (s, 3H), 4.21 (t, $J = 8.3$ Hz, 2H), 6.86 (d, $J = 8.6$ Hz, 2H), 7.00–7.24 (m, 2H), 7.33–7.43 (m, 2H), 7.51–7.70 (m, 1H). LCMS-ESI ($M + H$) $^+$: 341.0. HRMS (ESI): calcd for $\text{C}_{20}\text{H}_{25}\text{N}_2\text{OS}^+$, 341.1682; found, 341.1677.

1-(4-Phenoxybutyl)-1H-imidazole.



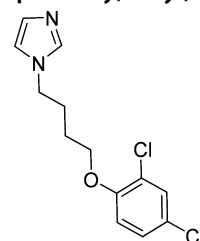
Compound **59**: LCMS-ESI ($M + H$) $^+$: 217.0, $t_R = 0.759$ min, purity >99%.

1-(4-(4-Chlorophenoxy)butyl)-1H-imidazole.



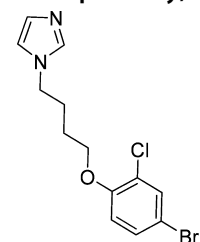
Compound **60**: LCMS-ESI ($M + H$) $^+$: 250.9, $t_R = 0.688$ min, purity 92%.

1-(4-(2,4-Dichlorophenoxy)butyl)-1H-imidazole.



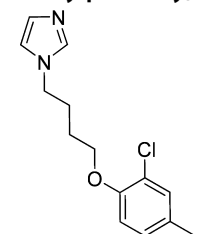
Compound **61**: LCMS-ESI ($M + H$) $^+$: 284.8, $t_R = 0.662$ min, purity 85%.

1-(4-(4-Bromo-2-chlorophenoxy)butyl)-1H-imidazole.



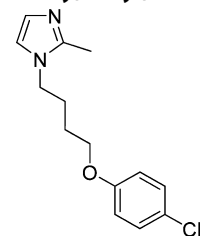
Compound **62**: LCMS-ESI ($M + H$) $^+$: 330.7, $t_R = 4.032$ min, purity 95%.

1-(4-(2-Chloro-4-methylphenoxy)butyl)-1H-imidazole.



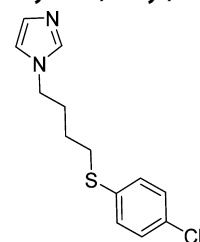
Compound **63**: LCMS-ESI ($M + H$) $^+$: 264.9, $t_R = 0.667$ min, purity >99%.

1-(4-(4-Chlorophenoxy)butyl)-2-methyl-1H-imidazole.



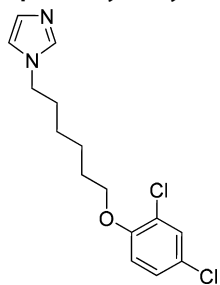
Compound **64**: LCMS-ESI ($M + H$) $^+$: 264.9, $t_R = 3.716$ min, purity 95%.

1-(4-(4-Chlorophenylthio)butyl)-1H-imidazole.



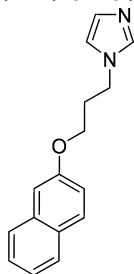
Compound **65**: LCMS-ESI ($M + H$) $^+$: 266.9, $t_R = 3.559$ min, purity >99%.

1-(6-(2,4-Dichlorophenoxy)hexyl)-1H-imidazole.



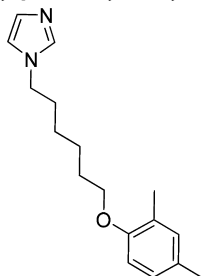
Compound 66: LCMS-ESI (M + H)⁺: 312.8, t_R = 4.441 min, purity 95%.

1-(3-(Naphthalen-2-yloxy)propyl)-1H-imidazole.



Compound 67: LCMS-ESI (M + H)⁺: 252.9, t_R = 3.667 min, purity >99%.

1-(6-(2,4-Dimethylphenoxy)hexyl)-1H-imidazole.



Compound 68: LCMS-ESI (M + H)⁺: 273.0, t_R = 4.391 min, purity 95%.

AUTHOR INFORMATION

Corresponding Author

*Phone: 206 858 6074. Fax: 206 381 3678. E-mail: tanya.parish@idri.org.

ORCID

Tanya Parish: 0000-0001-7507-0423

Author Contributions

N.S.C., B.J.B., G.S., T.O'M., A.M., L.F., and T.R.I. conducted experimental work. N.S.C., B.J.B., G.S., S.C., T.O'M., A.M., L.F., T.R.I., J.S., T.M., P.A.H., J.O., and T.P. conceived and designed the experiments and analyzed the data. N.S.C., B.J.B., G.S., S.C., J.O., and T.P. wrote the paper.

Notes

The authors declare no competing financial interest.

ACKNOWLEDGMENTS

We thank Alfredo Blakeley, James Ahn, Mai Ann Bailey, Jack Elder, Megan Files, Stephanie Florio, Julianne Olinger, Aaron Korkegian, and Yulia Ovechkina for technical assistance. Research reported in this publication was supported by NIAID of the National Institutes of Health under Award Number

R21AI107626 and the Bill & Melinda Gates Foundation, under Grant Numbers OPP1024038 and OPP1024055.

REFERENCES

- (1) WHO. (2016) *Global Tuberculosis Report*, http://www.who.int/tb/publications/global_report/en/.
- (2) Chandrasekera, N. S., Alling, T., Bailey, M. A., Files, M., Early, J. V., Ollinger, J., Ovechkina, Y., Masquelin, T., Desai, P. V., Cramer, J. W., Hipskind, P. A., Odingo, J. O., and Parish, T. (2015) Identification of Phenoxyalkylbenzimidazoles with Antitubercular Activity. *J. Med. Chem.* 58 (18), 7273–85.
- (3) Cook, G. M., Hards, K., Vilcheze, C., Hartman, T., and Berney, M. (2014) Energetics of respiration and oxidative phosphorylation in mycobacteria. *Microbiol. Spectrum* 2, 3.
- (4) Fry, M., and Pudney, M. (1992) Site of action of the antimalarial hydroxynaphthoquinone, 2-[trans-4-(4'-chlorophenyl) cyclohexyl]-3-hydroxy-1,4-naphthoquinone (S66C80). *Biochem. Pharmacol.* 43 (7), 1545–53.
- (5) Ortiz, D., Forquer, I., Boitz, J., Soysa, R., Elya, C., Fulwiler, A., Nilsen, A., Polley, T., Riscoe, M. K., Ullman, B., and Landfear, S. M. (2016) Targeting the cytochrome bc1 complex of *Leishmania* parasites for discovery of novel drugs. *Antimicrob. Agents Chemother.* 60 (8), 4972–82.
- (6) Abrahams, K. A., Cox, J. A., Spivey, V. L., Loman, N. J., Pallen, M. J., Constantinidou, C., Fernandez, R., Alemparte, C., Remuinan, M. J., Barros, D., Ballell, L., and Besra, G. S. (2012) Identification of novel imidazo[1,2-a]pyridine inhibitors targeting *M. tuberculosis* QcrB. *PLoS One* 7 (12), e52951.
- (7) Moraski, G. C., Seeger, N., Miller, P. A., Oliver, A. G., Boshoff, H. I., Cho, S., Mulugeta, S., Anderson, J. R., Franzblau, S. G., and Miller, M. J. (2016) Arrival of Imidazo[2,1-b]thiazole-5-carboxamides: potent anti-tuberculosis agents that target QcrB. *ACS Infect. Dis.* 2 (6), 393–8.
- (8) Pethe, K., Bifani, P., Jang, J., Kang, S., Park, S., Ahn, S., Jiricek, J., Jung, J., Jeon, H. K., Cechetto, J., Christophe, T., Lee, H., Kempf, M., Jackson, M., Lenaerts, A. J., Pham, H., Jones, V., Seo, M. J., Kim, Y. M., Seo, M., Seo, J. J., Park, D., Ko, Y., Choi, I., Kim, R., Kim, S. Y., Lim, S., Yim, S. A., Nam, J., Kang, H., Kwon, H., Oh, C. T., Cho, Y., Jang, Y., Kim, J., Chua, A., Tan, B. H., Nanjundappa, M. B., Rao, S. P., Barnes, W. S., Wintjens, R., Walker, J. R., Alonso, S., Lee, S., Kim, J., Oh, S., Oh, T., Nehrbass, U., Han, S. J., No, Z., Lee, J., Brodin, P., Cho, S. N., Nam, K., and Kim, J. (2013) Discovery of Q203, a potent clinical candidate for the treatment of tuberculosis. *Nat. Med.* 19 (9), 1157–60.
- (9) Gengenbacher, M., Rao, S. P., Pethe, K., and Dick, T. (2010) Nutrient-starved, non-replicating *Mycobacterium tuberculosis* requires respiration, ATP synthase and isocitrate lyase for maintenance of ATP homeostasis and viability. *Microbiology* 156 (1), 81–7.
- (10) Arora, K., Ochoa-Montano, B., Tsang, P. S., Blundell, T. L., Dawes, S. S., Mizrahi, V., Bayliss, T., Mackenzie, C. J., Cleghorn, L. A., Ray, P. C., Wyatt, P. G., Uh, E., Lee, J., Barry, C. E., 3rd, and Boshoff, H. I. (2014) Respiratory flexibility in response to inhibition of cytochrome C oxidase in *Antimicrob. Agents Chemother.* 58 (11), 6962–5.
- (11) Shi, L., Sohaskey, C. D., Kana, B. D., Dawes, S., North, R. J., Mizrahi, V., and Gennaro, M. L. (2005) Changes in energy metabolism of *Mycobacterium tuberculosis* in mouse lung and under in vitro conditions affecting aerobic respiration. *Proc. Natl. Acad. Sci. U. S. A.* 102 (43), 15629–34.
- (12) Lamprecht, D. A., Finin, P. M., Rahman, M. A., Cumming, B. M., Russell, S. L., Jonnal, S. R., Adamson, J. H., and Steyn, A. J. (2016) Turning the respiratory flexibility of *Mycobacterium tuberculosis* against itself. *Nat. Commun.* 7, 12393.
- (13) Ioerger, T. R., Feng, Y., Ganesula, K., Chen, X., Dobos, K. M., Fortune, S., Jacobs, W. R., Jr., Mizrahi, V., Parish, T., Rubin, E., Sasseti, C., and Sacchettini, J. C. (2010) Variation among genome sequences of H37Rv strains of *Mycobacterium tuberculosis* from multiple laboratories. *J. Bacteriol.* 192 (14), 3645–53.
- (14) Ollinger, J., Bailey, M. A., Moraski, G. C., Casey, A., Florio, S., Alling, T., Miller, M. J., and Parish, T. (2013) A dual read-out assay to evaluate the potency of compounds active against *Mycobacterium tuberculosis*. *PLoS One* 8 (4), e60531.

(15) Lambert, R. J., and Pearson, J. (2000) Susceptibility testing: accurate and reproducible minimum inhibitory concentration (MIC) and non-inhibitory concentration (NIC) values. *J. Appl. Microbiol.* 88 (5), 784–90.

(16) Ford, C., Yusim, K., Ioerger, T., Feng, S., Chase, M., Greene, M., Korber, B., and Fortune, S. (2012) *Mycobacterium tuberculosis*—heterogeneity revealed through whole genome sequencing. *Tuberculosis (Oxford, U. K.)* 92 (3), 194–201.

(17) Darby, C. M., Ingolfsson, H. I., Jiang, X., Shen, C., Sun, M., Zhao, N., Burns, K., Liu, G., Ehrst, S., Warren, J. D., Anderson, O. S., Brickner, S. J., and Nathan, C. (2013) Whole cell screen for inhibitors of pH homeostasis in *Mycobacterium tuberculosis*. *PLoS One* 8 (7), e68942.

(18) Manning, A. J., Ovechkina, Y., McGillivray, A., Flint, L., Roberts, D. M., and Parish, T. (2017) A high content microscopy assay to determine drug activity against intracellular *Mycobacterium tuberculosis*. *Methods (Amsterdam, Neth.)* 127, 3–11.

(19) Zelmer, A., Carroll, P., Andreu, N., Hagens, K., Mahlo, J., Redinger, N., Robertson, B. D., Wiles, S., Ward, T. H., Parish, T., Ripoll, J., Bancroft, G. J., and Schaible, U. E. (2012) A new *in vivo* model to test anti-tuberculosis drugs using fluorescence imaging. *J. Antimicrob. Chemother.* 67 (8), 1948–60.